Indian J. Phys. **66A** (1 & 2) 37–89 (1992)

Oxide glass to high temperature ceramic superconductors — a novel route

B K Chaudhuri* and K K Som
High Temperature Superconductivity Laboratory,
Solid State Physics Department,
Indian Association for the Cultivation of Science,
Calcutta–700 032, India

Abstract : The transition metal oxide (TMO) glasses are highly interesting because of their applications in switching and memory devices, batteries, storage of nitrogen for agricultural uses etc. Recently it has been discovered that many of these oxide glasses like Bi-Sr-Ca-Cu-O, Y-Ba-Cu-O, Bi-Pb-Sr-Ca-Cu-O etc. can be directly converted to the corresponding high temperature superconducting phases by properly annealing the respective glasses. In this review article we have attempted to summarize the very recent developments in this field of immense technological importance. The structural, electrical, dielectric, magnetic, optical, and other properties of these new type of (TMO) glass systems have been elucidated comparing them with the corresponding results of already known (TMO) glasses which do not become superconductors upon annealing above their glass transition temperatures (T_g). The electrical properties of this novel glass system of our present discussion have been analysed with reference to the various existing theoretical models based on polaron hopping conduction mechanism. The electrical, magnetic, and other properties of the respective superconductors obtained from their corresponding glass phases by annealing above (T_g) have also been discussed. Finally, the possibility of drawing wires, ribbons etc. from these glass matrices and then converting them to their high T_c superconducting phases have been discussed for encouraging further developments in this direction.

Keywords : High temperature superconductors, transition metal oxide glasses, polaron model

PACS Nos : 74.30.–e, 74.70.Mq

1. Introduction

The transition metal oxide glasses (TMOG) have been widely studied because of their interesting physical properties as well as for their applications in switching and memory devices [1–2], cathode-ray tube materials [3], ferrites [4], etc. These glasses have also important semiconducting properties which arise due to the presence of transition metal ions (TMI) in more than one valence states in the glass materials [5–10]. In these glasses

*Author for correspondence
Text as per authors' format

the electron-phonon interaction is strong enough to form small polarons and the electrical conduction occurs by the hopping of small polarons from the ion of low valency state to the ions of high valency state of the TMI's [6]. It is also observed from the literature survey that vanadium and iron oxide glasses [1–12] have been studied more extensively than the other TMI glasses, such as copper oxide glasses [7, 13–17]. Drake and co-workers [13] first reported the DC conductivity and switching in the P_2O_5 – CaO – CuO and in B_2O_3 – CaO – CuO glasses. The conduction process in these copper oxide glasses are characterized by a high activation energy (~1 eV) [7, 13, 15, 16] which is mainly governed by an electron hopping mechanism between non-identical Cu–sites. The activation energy was too large to be explained by polaronic hopping conduction as observed in vanadium and iron oxide glasses [1–12]. It was pointed out by Austin and Mott [6] that the ligand field environment is different for Cu^+ and Cu^{2+} ions and thus part of the activation energy can be a carrier excitation energy from one site to another. In addition, these glasses can be switched to a higher conduction state with a lower activation energy (~0.015 eV). In this state the site environments are not identical. Moreover, it seems that polaron energy does not exist due to large radial extension of the copper ion wavefunction. Drake and Scanlan [14] proposed that Cu^+ and Cu^{2+} ions exist in different coordination spheres in copper glasses. They also proposed that the energy level exension of these states is enough to produce some overlapping, which provides polaron hopping conduction in those overlapped levels. Some authors [17] also postulated a mixed electronic and ionic conductivity in copper-phosphate glasses and this behaviour is interpreted by assuming that the Cu^+ ion exists in sites with different bonding forces.

Recently copper containing semiconducting oxide glasses like $Y_1Ba_2Cu_3O_x$ (1:2:3) [18-20], $Bi_4Sr_3Ca_3Cu_4O_x$ (4:3:3:4) [21–26], etc. have been discovered. These glasses are very interesting because they could be converted into high temperature superconducting oxide (HITSO) phases by properly annealing them in air or in flowing oxygen atmosphere (hereafter referred to as "galss to ceramic route", GCR). This is a new technique for making (HITSO) with the following advantages .

(a) The HITSO obtained by GCR is extremely dense compared to those obtained by the usual ceramic sintering or chemical methods.

(b) Since the glass samples are thoroughly mixed and melted, one might get highly homogeneous (HITSO) materials.

(c) It is well known that the superconducting critical current density (J_c), depends on the proper orientations of the crystallites. Using the (GCR) technique the microstructures of the crystalline (HITSO) materials could be highly controlled and hence the J_c values could be increased.

(d) The nucleation and growth processes of both the 85K and 110K (HITSO) phases of the Bi–Sr–Ca–Cu–O system, for instance, have not yet been studied. The complicated intergrowth of the 110K phase is difficult to study

with ceramic sintered sample, since the microstructures are not easily controlled in this process. In the liquid quenched oxide glasses, on the other hand, the starting material has a highly uniform and dense amorphous structure, and the crystallization can be carefully controlled by adjusting the annealing parameters. The complete phase change process can, therefore, be clearly observed by various characterization techniques [27, 28].

(e) The glass transition temperature (T_g), crystallization temperature (T_x) and hence the superconducting transition temperature (T_c) of a sample could be changed, if required, by adding different atoms in the glass compositions.

(f) The prepared superconductors posses properties such as phase purity, absence of defects, high density, chemical stability, and oriented microstructures.

(h) The glass to ceramic technique has also great significance because it might be possible to make (HITSO) wires, tapes or fibers and films using this technique [23, 29–31].

Table 1A. Some characteristic parameters of ($Y_1Ba_2Cu_3O_x$) glass and superconductor (B : Bulk, W : Wire or Tape, F : Film)

Samples	T_g, T_x, T_m °C	T_c/T_{co} K	J_c A/cm^2	Properties studied	Reference
(1:2:3) (B)	—		—	Annealing around 850°C, XRD, DTA, SEM, χ (susceptibility)	[19]
(1:2:3) (B) with MgO	—	T_c = 90 (70-75) with MgO)	—	Annealing around 900°C, χ, SEM R (resistivity)	[99]
(1:2:3) (b) with B_2O_3	—	T_c = 80.5	—	R, χ, XRD	[100]
(1:2:3) (B)	—	—	> 10^4	SEM	[98]
(1:2:3) (b)	—	93/88	—	R, AC Josephson effect at 77K	[18]
(1:2:3) (F) on MgO (100) plane	—	T_c = 95	—	SEM, XRD	[30]
(1:2:3) (F) 50 μm	—	95/87	—	XRD, R	[14]
(1:2:3) (B)	—	92/89	—	R. XRD, glass density = 5.41 g/cm^3 annealed density = 5.17 g/cm^3	[18]

Quite high value of T_c was obtained by this GCR process. Ibara *et al* [32] and Komatsu *et al* [24, 33–35] prepared (HITSO) with critical temperature T_c above 110K from the Bi–

Pb–Sr–Ca–Cu–O glass system. Recently Shi *et al* [26] also reported that $Bi_2Sr_2Ca_3Cu_4O_x$ and $Bi_2Sr_2Ca_4Cu_5O_x$ glasses exhibit superconductivity with $T_c > 100K$ when annealed at 870°C for several days in air. In Table 1 we have listed the different Bi and Y–based oxide glasses and ceramics having their different glassy and superconducting properties.

Table 1B. Some characteristic parameters of $(Bi_uSr_vCa_wCu_yO_x)$ type glasses and superconductors (B · Bulk, F Films or Tapes, W Wires or Rods)

Samples (u·v:w:r)	T_g/T_x °C	T_c/T_∞ K	J_c A/cm^2	Properties studied	Reference
(1.2 3) (B)	$T_g = 435$	98/93	35 at 77K	XRD, χ, R DTA	[65, 24, 50, 103, 73]
(2 2 1:2) (F)	$T_x = 486$	~ 88			
(2.2·1.2) (F)	$T_x = 733K$	86.8, 98/	—	R, XRD,	[31, 65]
	$T_g = 700K$	66.7, 93		DTA, TGA	
(1.1·1:2) (B)	$T_g = 390$,	102–110/	102	XRD, SEM,	[27, 46, 47,
	680K	80–91	at 77K	TGA, DTA, χ,	35, 53, 61,
	$T_x = 444$		220	Hall, C_P,	103, 49]
			at 4.2K	Sp. heat	
(4:3:3 4) (B,F)	$T_x - T_g$	85/80, 101	15	XRD, R, χ,	[52, 23, 48,
(4·3:3·y) (B)			at 77K	SEM	22, 67, 51]
(y:3:3:4) (B)					
y = 2 5 – 5.5					
(1.3.1.1.2)	$T_g = 680K$	—	—	Sp heat,	[49]
	$T_x = 725K$			electron micrograph	
(2.2:2.3)	—	110/80	—	SEM, DTA, R	[54]
(1:1:1:2)	$T_g = 390$	$T_g = 88$	—	XRD, DTA,	[24, 22]
				TGA, R	
(2:0.6.1.4:2)	—	115/80	—	XRD, EDX	[73]
(2.2·1.2)				SEM, R	
(1.5:1:1.5:2)	$T_g = 425$	95–80/	—	XRD, R	[35, 28]
(B)	$T_g = 670K$	78–63		DTA, DSC	[104]
	$T_x = 725K$				
(2 1:1:1:1.2)	$T_x \sim 720K$	—	—	DSC, R	[50, 55]
(B)				dielectric const.	

All these findings definitely drew attention of many scientific workers to the glass–ceramic route for obtaining (HITSO) materials in different forms. In this review we have, therefore, made a thorough analysis of the method of preparation of different Y– and Bi–based (TMI) glasses, their characterizations investigating the electrical, magnetic, dielectric,

infrared, and other properties in one hand, and the process of converting these glasses in the corresponding (HITSO) analogue and the studies of their superconducting properties, on the other hand. Detailed studies of the electrical and magnetic properties of the glass phases would help to understand why these types of glasses become superconductor when annealed. Finally, the possibility of making (HITSO) wires, tapes, and films using the GCR technique have also been enlightened.

Table 1C. Some characteristic parameters of ($Bi_uPb_vSr_wCa_tCu_rO_x$) glass and superconductor (B : Bulk, W : Wire or Tape, F : Film)

Samples (u:v:w:t:r)	T_g, T_x, T_m ^{0}C	T_c/T_{co} K	J_c A/cm^2	Properties studied	Reference
(0.96:0.24:1:1:1.8) (B)	—	T_c = 110	—	R, χ', χ'', variation of T_c with quenching temperature	[68]
(0.8:0.2:1:1:2) (B)	—	T_c = 100	120 at 77K	R, χ, XRD, DTA	[34]
(0.7:0.3:1:1:1.8) (B)	T_m = 1200	115/ 105	—	SEM, χ, R	[69]
(1;y1:1:2) (B) (y = 0, 1-0, 4)	T_g = 480	T_c =120–115 T_{co} = 92–82	—	R, XRD, DTA	[32]
(0.8:0.2:1:1:2) (B)	—	T_{co} = 100	35-36 at 77K	XRD, R,	[101]
(1.5:0.5:2.2:3) (B)	T_g = 383 T_x = 446 T_m ~ 855	109/ 107	—	Annealing time and temperature dependence of T_c	[64]
(1.6:0.4.2:2:3) (B)	T_g = 620K T_x = 720K	—	—	DTA, DSC	[55]

2. Preparation of glasses

Amorphous solids are prepared, in general, by two ways : (1) by condensation from the vapour phase as in thermal evaporation, sputtering, glow discharge decomposition of a gas or other methods of deposition [36–37], and (2) by cooling from a melt [38–40]. The first method produces thin films and the second bulk materials. If a material can be prepared in the amorphous phase from a melt, it is generally also possible to prepare it.by deposition. However, there will inevitably be some structural differences between the samples of same material prepared by different methods, which must be taken into consideration in any comparative study of physical properties. Other methods include electrolytic deposition from solution, and prolonged irradiation of crystalline materials with high energy particles such as neutrons or ions. A general review describing these methods of preparing amorphous solids has been reported by Owen [41].

Several transition metal oxide glasses when heated with glass forming oxides like P_2O_5, TeO_2, GeO_2, Bi_2O_3 etc. form semiconducting glasses on quenching the melt [5–10] below the glass transition temperature T_g. The second order thermodynamic quantities such as the thermal expansion coefficient, specific heat etc. show a discontinuous change at T_g (Figure 1). It is also observed from Figure 1b that the glass transition temperature is not particularly well defined, unlike the melting point T_m of the crystal. The transition temperature is not sharp but occurs over a range of temperatures. For the glasses of our present interest, this behaviour of the glass transition is also recognized.

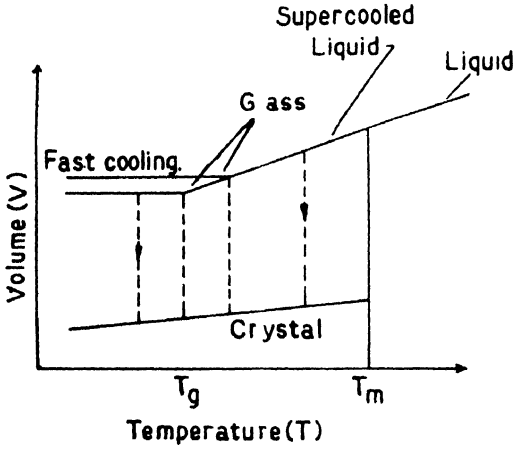

Figure 1.(a) Schematic variation of volume versus temperature of a glass forming material.

The method of obtaining amorphous solid by cooling the melt can yield homogeneous amorphous solids only when the melt is cooled above a certain critical cooling rate r_c [42] given by

$$r_c = 2.0 \times 10^6 T_m^2 R'/V\eta \tag{1}$$

where R' is the gas constant, V is the volume, and η is the viscosity of the material in the melt. The glass will be in the metastable equilibrium if it is brought to that temperature instantaneously. Furthemore, T_g depends on the cooling rate and subsequent thermal history (Figure 1b). If the glass is kept at temperature much lower than T_g, it will be stable for all practical purposes. For this, to study the properties of the glasses, one should anneal the glass samples well below the glass transition temperature (properties of the new type of glasses of our interest are discussed in Sec. 4). Heat treatment near T_g may change the physical properties of glasses due to crystallization and hence superconducting phase might appear along with the glass samples. Several model-based theoretical approaches such as free volume theory [43], entropy theory [44], bond lattice model theory [45] etc. have been developed to understand the glass transition phenomenon.

The preparation techniques and behaviour of the oxide glasses (as shown in Table 1) of our present interest are also found to follow the general behaviour of the (TMI) oxide glasses discussed above. For instance, the glasses like $Bi_4Sr_3Ca_3Cu_4O_x$ (4:3:3:4) [23] are

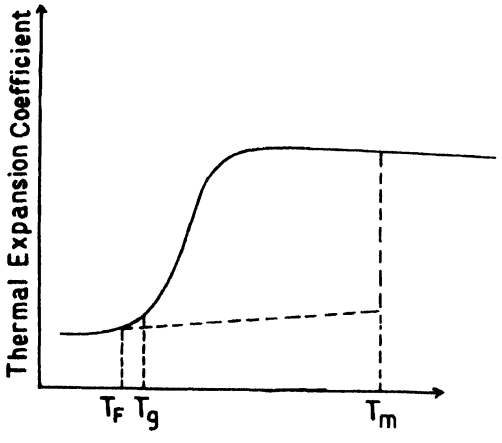

Figure 1.(b) Variation of thermal expansion coefficient with temperature of a glass.

prepared by mixing appropriate amount of Bi_2O_3 , $SrCO_3$, $CaCO_3$, and CuO and then melting the mixture in air in an alumina (or platinum) crucible. The melt is then quenched by pressing the cast liquid between two polished copper or stainless steel blocks kept at room temperature. For making homogeneous glass it is necessary to stir the melt occasionally with a platinum rod. Moreover, before melting the oxide mixtures ($SrCO_3$, $CaCO_3$, Bi_2O_3 and CuO) it is also necessary to sinter them in air at about 800°C for 8–10 hours and then to cool the mass slowly to room temperature. This is also necessary to minimise the evaporation loss during melting. This powder is regrinded and melted at 1000–1100°C for two to three hours for making homogeneous glass which is dark red with metallic lusture.

Skumryev *et al* [46] used oxy-acetylene flame for making the glasses. Some other similar methods like laser melting, Xe-arc imaging furnace [31] etc. have also been used for the purpose of making homogeneous glasses. The quenching rate of the glass is about 10^5K/s.

Murakami *et al* [20], and Komatsu *et al* [18, 33-35] also reported similar preparation technique for making $YBa_2Cu_3O_x$ glasses which could also be tramsformed to (HITSO) phase by properly annealing its glass phase. The starting materials for the $YBa_2Cu_3O_x$ (1:2:3) glasses being Y_2O_3, $BaCO_3$, and CuO. The purity of the starting materials being 99.99% or better. It has already been pointed out that in this melt quenching process homogeneous mixture of the melt is very important to get a homgeneous glass

composition. The melt of these glasses are just like liquid water. This is way it is rather difficult to make wires or tapes directly from their melts unlike the vanadate type of glasses. However, addition of some amount of B_2O_3, increase of Bi_2O_3 content, melting the glass in presence of inert atmosphere etc. might make it possible to draw wires or tapes from these glasses. We shall discuss this point at the end of this review. One should also notice the loss of weight of the sample during melting. For a typical example, the weight loss of the $Bi_2Sr_2CaCu_2O_x$ (2:2:1:2) galss film [31] during melting is about 0.2 wt%. However, this weight loss also depends to some extent on the method of preparation. Proper care should, therefore, be taken while preparing the glass. The weight loss is mainly due to chemical changes as well as evaporation loss. All the oxide glasses thus prepared by different authors are semiconductors (Sec. 6.2) like other TMI oxide glasses [7].

The prepared glasses are characterized by differential thermal analysis (DTA), thermogravimetric analysis (TGA), differential scanning calorimetry (DSC), X–ray diffraction (XRD), scanning (SEM) and transmission (TEM) electron microscopy, atomic absorption, energy dispersive X–ray analysis (EDXA) etc. as discussed below.

3. Characterizations of the glasses

If proper care, as mentioned in Sec. 2, is taken, the glasses prepared by melt quenching would be homogeneous and mostly of single phase in character. In some cases formation of a $Bi_2Sr_2Ca_{n-1}Cu_nO_x$ intermetallic compound with high melting point (T_m = 1200°C) creates problem to get single phase compound [21]. Some additional XRD peaks of the CaO, $CaCu_5$, $Bi_{10}Ca_{11}$, Cu, Bi etc. are also sometimes detected by several authors in the glassy as well as in the corresponding superconducting phases with different superconducting trasition temperature (T_c) [21, 47]. However, homogeneous single glass samples have also been prepared by several authors [22-25, 48, 49] for which proper mixing of the melt constituents, control of melting temperature, and high quenching rate of the melt are necessary.

3.1. X–ray diffraction and SEM studies :

The XRD patterns with CuKα radiation of some of the Bi-based glasses are shown in Figure 2. These diffraction patterns of the rapidly quenched glasses show only broad diffuse peaks without showing any crystalline structure. This indicates that the glasses are homogeneous and are of single phases. However, depending on the quenching rate, heating temperature etc. as mentioned in Section 2, some crystalline peaks might also be observed [18, 50]. This type of samples showing a few crystalline peaks would also be superconducting upon annealing having a little lower T_c value (or indicating the presence of both high T_c and low T_c phases in the annealed samples). For these samples anomalies in the electrical resistivity and magnetic susceptibility are also expected. However, large differences in the electrical and other properties of this glass from those of the single phase pure oxide glass of same composition are always envisaged for obvious reasons.

The magnitudes of the scattering vector defined by $S_k = 4\pi \sin\theta/\lambda$ at the peaks of the X-ray diffractograms were found to vary slightly between 20.6 to 21.0 nm^{-1} for the Bi-based oxide glasses. The glassy nature of the samples was also confirmed from the SEM

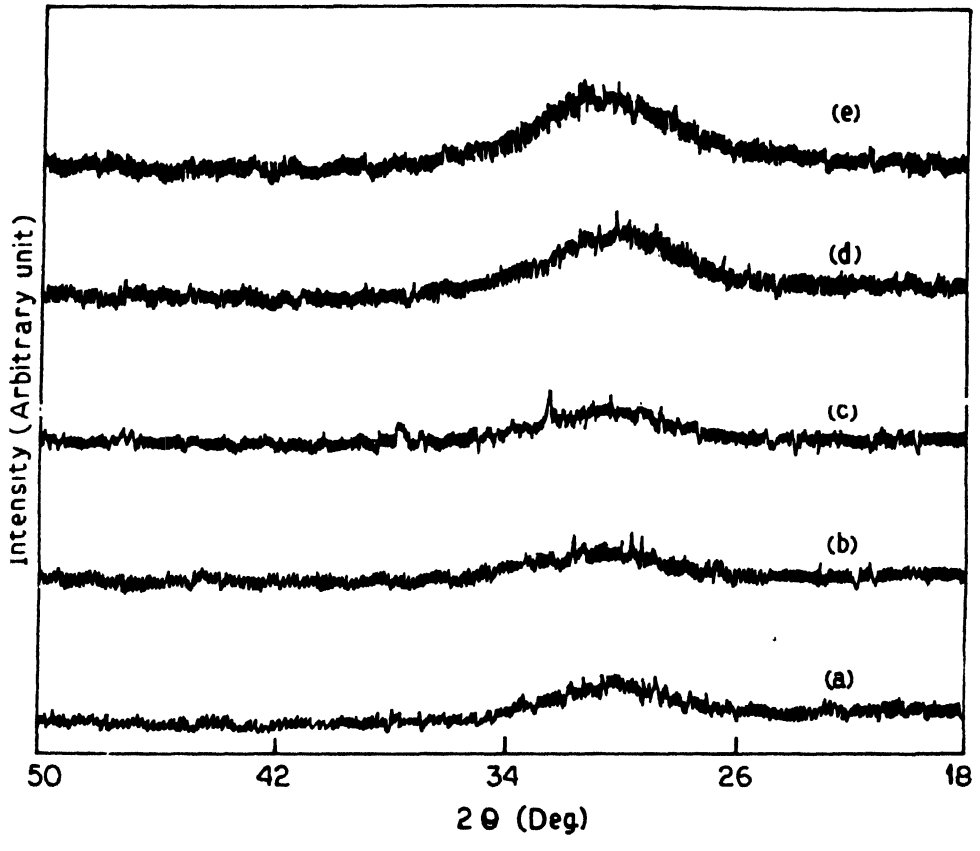

Figure 2. X-ray diffraction patterns of some ($Bi_4Sr_3Ca_3Cu_yO_x$) type glasses (a : y = 3, b : y = 3.5, c : y = 4, d : y = 4.5, e : y = 5).

and TEM studies [23, 49]. Some of the SEM pictures for the (4:3:3:4) glasses are shown in Figure 3 which clearly indicate the glassy behaviour of the samples. For most of Bi-based glasses a broad hump extending between $2\theta = 20 - 40$ degrees are observed for different compositions of the glasses [22, 23, 32, 50]. From X-ray analysis no evidence of the superconducting phase in the glass sample is observed. However, some indication of the presence of the high T_c superconducting phase in the glass sample has been reported from

microwave absorption study [50]. It would be interesting to observe this superconducting phase in the glass from other expeimental studies.

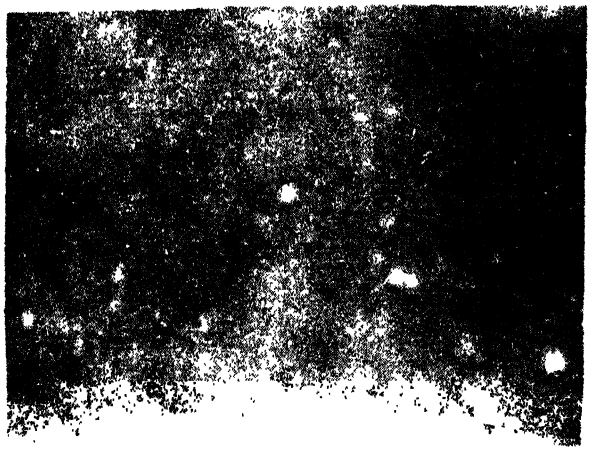

(a)

Figure 3. Scanning electron micrographs of a ($Bi_4Sr_3Ca_3Cu_4O_x$) glass showing phase separation for low temperature which disappears for high temperature long time annealing. (a : original quenched glass,

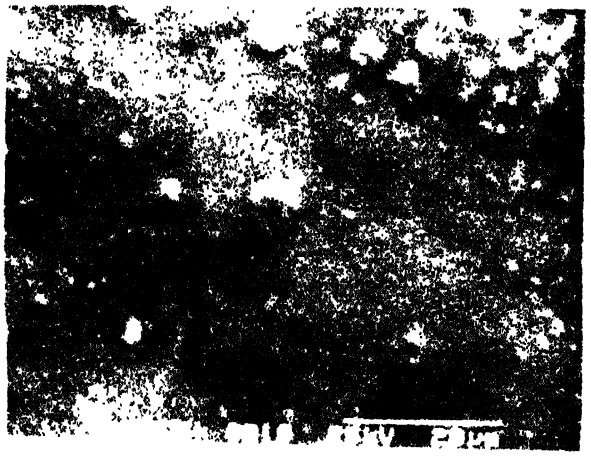

(b)

Figure 3. Scanning electron micrographs of a ($Bi_4Sr_3Ca_3Cu_4O_x$) glass showing phase separation for low temperature which disappears for high temperature long time annealing. b : annealed at 200°C for 2 h,

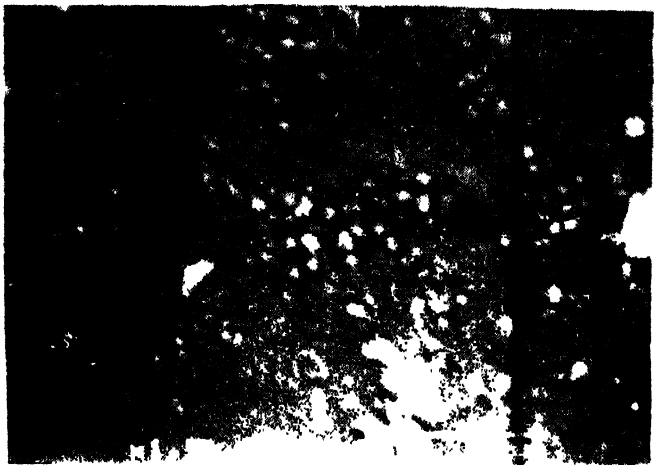

(c)

Figure 3. Scanning electron micrographs of a ($Bi_4Sr_3Ca_3Cu_4O_x$) glass showing phase separation for low temperature which disappears for high temperature long time annealing. (c : annealed at 400°c for 10 h).

3.2. Density of glasses :

It is to be noted that the initial glass phase is about 100% dense with no noticeable voids present as observed from SEM studies [51, 52]. It has also been observed that the densities (ρ) of the annealed glasses (i.e. superconducting phases) is much higher than those of similar samples obtained by usual solid state reaction (SSR) routes. This is one of the important features of the (GCR) technique of making (HITSO) from oxides as mentioned above. Some interesting variations of the density of these glasses with the variations of CuO and Bi_2O_3 concentrations have been shown in Figure 4. This figure shows that the density of the $Bi_ySr_3Ca_3Cu_4O_x$ (y = 5, 4.5, 4, 3.5, and 3) glasses first increases with the increase of Bi_2O_3 concentrations and then it decreases for more than 15 mol % of Bi_2O_3. This behaviour of density is similar to the variation of density of the CuO–BaO–P_2O_5 glass [13] with CuO concentration. For $Bi_4Sr_3Ca_3Cu_yO_x$ glass, on the other hand, the density of the glasses decreases with the increase of CuO concentrations which is similar to the behavior of density of the Bi_2O_3–Fe_2O_3 glasses [12].

The apparent molar volume of oxygen (V^*) of the (4:3:3:y) glasses, for example can be calculated approximately using standard relation

$$V^* = \text{molecular wt./density x } W_o \qquad (2)$$

where W_o is the number of oxygen atoms in the formula unit. The variation of V^* with CuO concentration is also shown in Figure 4 for the (4:3:3:y) glasses. The quasi linear variation of V^* with CuO concentrations suggests that the geometry and topology of the random network is not changing largely with compositions in these glasses. This is also

supported from the fact that the superconducting transition temperatures T_c for these (4:3:3:4:y) glasses do not change drastically with CuO concentrations [51]. The change of slope of V^* with CuO concentrations (or the occurrence of an extremum in the curve) might

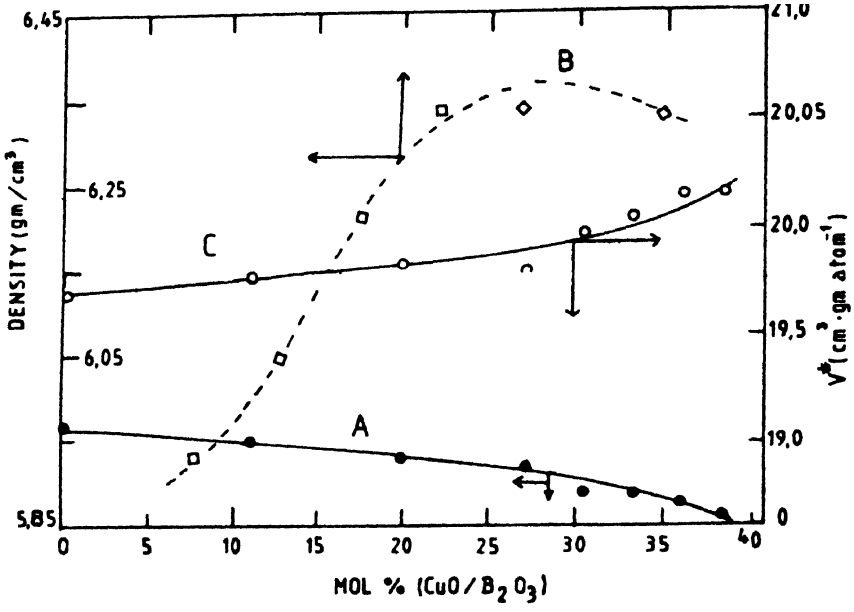

Figure 4. Variations of densities of the ($Bi_4Sr_3Ca_3Cu_yO_x$) and ($Bi_ySr_3Ca_3Cu_4O_x$) type glasses as a function of CuO (A) and Bi_2O_3 (B) mol%. Variation of apparent molar volume (V^*) of oxygen of ($Bi_4Sr_3Ca_3Cu_yO_x$) glass (*C*).

also indicate the existence of either composition dependent structural changes or phase separation in the glass. The phase separation in the (4:3:3:4) glass has really been observed by us as shown from the SEM pictures taken at different annealing temperatures [51]. The different phases are observed for low temperature annealing. These phases however, disappear when the samples are annealed for a long time at a higher temperatures above the glass transition temperatures (Figure 3).

3.3. DTA, TGA, and DSC studies on glasses :

The glass transition temperature (T_g) as well as crystallization temperature (T_x) of several glasses as studied by DTA are shown in Table 1. The DTA curves for some Bi-based glasses with heating rate of 10°C/min are shown in Figure 5 for comparison. The T_g values of the present glass system (Table 1) are relatively higher than the other Bi_2O_3 containing glasses which do not become superconductor upon annealing above the glass transition temperature [2, 11, 12]. The T_g values, however, decreases with the addition of Pb in the Bi-Sr-Ca-Cu-O systems (Table 1C). The T_g value of a typical Bi-Pb-Sr-Ca-Cu-O glass is about 395°C, while that for the Pb free Bi-Sr-Ca-Cu-O glass is about 480°C. However, the T_g and crystallization temperature T_x depend on the composition of the glasses (Table 1).

The oxygen released during melting of the glass sample is also indicatd from the TG analysis [27, 31, 48, 53]. The oxygen released seems to be recovered during annealing above 550°C. However, it might be pointed out that although the details of the structure in the DTA scan are different for different compositions of the glasses and also for the glass environment, most of the samples used for high temperature DTA study have some superconducting fraction present upon annealing at or around 830°C (even for a short time).

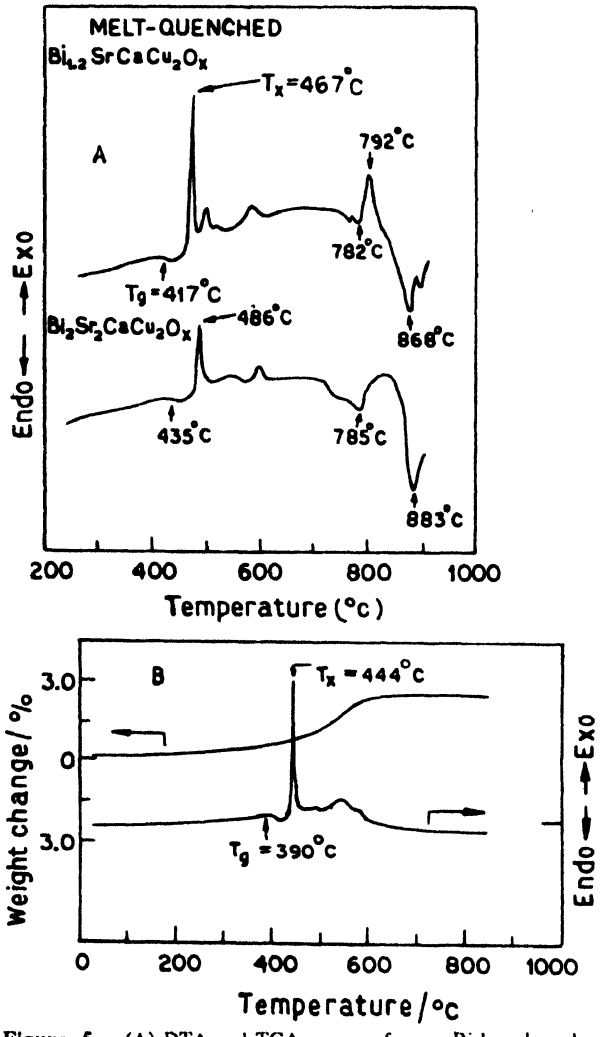

Figure 5. (A) DTA and TGA curves of some Bi-based oxide glasses ($Bi_{1.2}SrCaCuO_x$) and ($Bi_2Sr_2CaCu_2O_x$) [24], (B) DTA and TGA curves of $BiSrCaCu_2O_x$ glass [27].

Heating to higher temperature results in melting as observed by the large endotherm near 900°C. The DTA cooling curve after melting shows that these materials undergo incongruent melting as several exotherms are noted [54] in the temperature range where the initial melting takes place. However, the X-ray analyses show no evidence of the superconducting phase remaining in resolidified samples. This behaviour also appears to be

different from the usual oxide glass systems. As pointed out by Kanai *et al* [53], in the TGA curve the weight of the sample gradually increases from 500°C and has a maximum value around 750-850°C. Since the weight change is considered to be caused by the absorption and desorption of oxygen, the above increase mean that while going from the glass phase to the crystal phase more oxygen is needed.

Several reports of the differential scanning calorimetric (DSC) studies have also been made [28, 46, 49, 55]. Varma et al [55] showed from specific heat (C_p) data a single glass transition at $T_g \sim 650$K with crystallization temperature $T_x = 720$K for the ($Bi_2CaSrCuO_x$) glasses. The DSC thermogram for the ($Bi_1Sr_1Ca_1Cu_2O_x$) glass showed $T_g = 687$K (for a 10K/min warming rate [46]). Three overlapping exothermic peaks with a total heat of

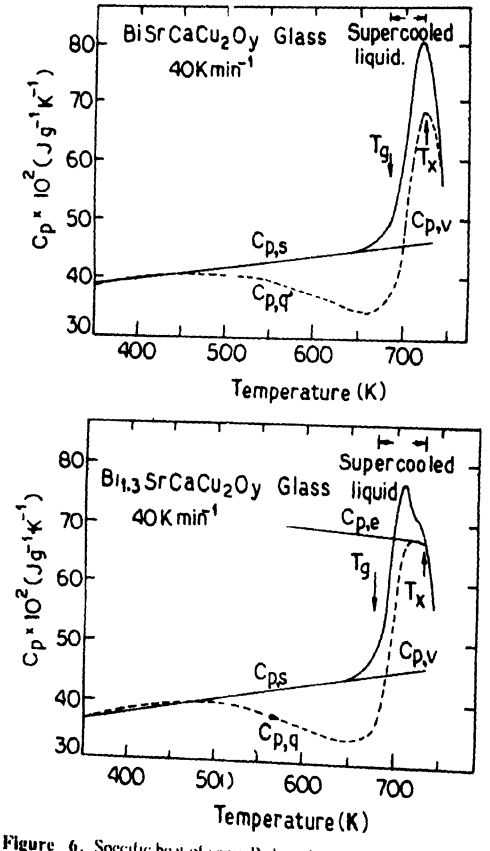

Figure 6. Specific heat of some Bi-based oxide glasses [49].

transformation of 13.6 cal/g are also observed for this glass at 734K, 745K, and 758K, respectively, indicating crystallization stages of the materials.

The specific heat (C_p) associated with structural relaxation, glass transition, and crystallization of a Bi-based glass was measured by Inoue *et al* [49] with a scanning

calorimeter. The thermogram of a $Bi_{1.3}SrCaCu_2O_y$ glass is shown in Figure 6. The quenched sample has $C_p = 0.38\ Jg^{-1}k^{-1}$ near room temperature. The C_p values increase with the rise of temperature and then begin to decrease indicating an irreversible structural relaxation at about 460K for the above glass. At the glass transition region ($T_g \sim 680K$) C_p increases rapidly and reaches an equilibrium liquid value of about $0.63\ Jg^{-1}k^{-1}$ around 718K (for $Bi_{1.8}SrCaCu_2O_y$) glasses. With further increase of temperature the supercooled liquid crystallizes around 725K for the ($BiSrCaCu_2O_y$) glass. For higher values of Bi in the glass, the T_g and the temperature of the supercooled liquid region decreases whereas T_x increases, indicating a clear tendency for the thermal stability of the glasses with higher concentration of Bi. The difference in C_p values between glassy solid and supercooled liquid reaches 0.283 $Jg^{-1}k^{-1}$ for ($BiSrCaCu_2O_y$) glass [49]. Therefore, the glassy structure in the Bi-Sr-Ca-Cu-O oxides is more stable than that of the heat treated crystallized smaples.

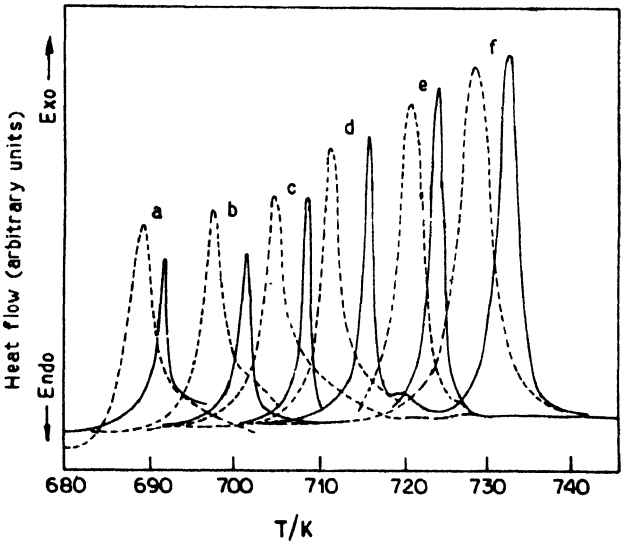

Figure 7. DSC curves of some Bi-based oxide glass [28]. Heating rates of (a) 1, (b) 2.5, (c) 5, (d) 10, (e) 20 and (f) 40 K/min.

The existence of the supercooled liquid over a relatively wide temperature range for the Bi-Sr-Ca-Cu-O type glasses might have important role for the development of (HITSO) wire from the glassy oxides. The equilibrium specific heat of the supercooled liquid C_{ps} can be appoximately calculated from

$$C_{ps} = A + B(T_x - T)\ Jg^{-1}k^{-1} \tag{3}$$

For a typical ($Bi_{1.3}SrCaCu_2O_x$) glass $A = 0.673$, $B = 10.7 \times 10^{-4}$ and $T_x = 730K$.

Tatsumisago and Angell [28] studied the crystallization kinetics for quenched ($Bi_{2.7}Ca_1Sr_1Cu_2O_x$) glass using a DSC. Figure 7 shows the DSC crystallization peaks at

different heating rates of the glass and the powder glasses. Here it is observed that for both the samples the exothermic peak shifted to higher temperatures with the increase of heating rates. Tatsumisago and Angell [28] also suggested surface crystallization as the dominant mechanism. The activation energy E_a for crystal growth may be calculated from the following relation [56] viz.

$$\log\left(\frac{\alpha^n}{T_p^2}\right) = -\frac{mE_a}{RT_p} + A \tag{4}$$

where α is th heating rate, T_p is the peak temperature (Figure 7), R is the gas constant, m and n are numerical factors depending on crystallization mechanisms. This calculation showed that the surface nucleation decreased with an increase in the Bi-content in the glass. Such a composition dependence is consistent with that of the activation energy for viscous flow in the glass transforming range and also influences the properties of the glasses and superconductors obtained from these glasses by annealing. Lowering of the Bi–content actually favours the glass formation but it lowers the T_c values of the superconductor.

In the $Bi_2(Ca, Sr)_{n+1}Cu_nO_{2n+4}$ series the formation of glasses with lower value of T_g and T_x corresponds, in general, to those glasses with lower n vaue ($n = 1$). The reaction mechanism for the formation of the glass from melt may also be written as

$$2\ Bi_2(Ca, Sr)_3Cu_2O_8 \quad \text{(melt)}$$

quenched

$$\longrightarrow\ Bi_2(Ca_2, Sr_2)CuO_6 \quad \text{(melt)} \qquad \text{(A)}$$

$$+\ Bi_2(Ca_4, Sr_4)Cu_3O_{10} \quad \text{(glass)} \qquad \text{(B)}$$

where $Bi_2(Ca_4, Sr_4)CuO_8$ is a semicoductor and $Bi_2(Ca, Sr)_4Cu_3O_{10}$ phase is stable in a restricted temperature rang 800-840°C. Above this limit it decomposes into other non-superconducting phases.

3.4 Infrared studies of glasses :

Infrared (IR) studies of a very few glass samples have been made [52, 57]. The general behaviour of IR absorption spectra of the (4:3:3:4) type glasses, for example, are the same as shown in Figure 8. Zheng *et al* [52] observed that there are four fundamental vibrational bands in the $BiO_{1.5}$-CuO-$Sr_{0.5}Ca_{0.5}$ corresponding to the frequencies = 840, 620, 500 and 300 cm^{-1}. The IR spectra of crystalline Bi_2O_3 [12] showed absorption bands at 360, 395, 450, 525, 610, 8700, 1400, 1480 and 1600 cm^{-1}. It, therefore, appears that there is a drastic change in the IR spectra of the Bi_2O_3 crystalline sample when it makes glass with CuO, SrO, and CaO. Zheng *et al* [52] concluded from the IR spectra that the glasses consist of $[Bi_2O_3]$ units in their glass network systems. More elaborate IR studies both at low and high temperature might be very interesting for these glasses.

4. Preparation of superconductor from glasses

The transformation of the glassy phase to the corresponding superconducting phase is a slow annealing process. The glasses (as shown in Table 1) are annealed in air or in oxygen atmosphere above the glass transition or the crystallization temperature (in the range of 800-830°C for the Bi–based glasses). The X–ray diffraction patterns of some annealed glasses are shown in Figure 9 indicating the presence of perfect crystallization peaks in their superconducting phases.

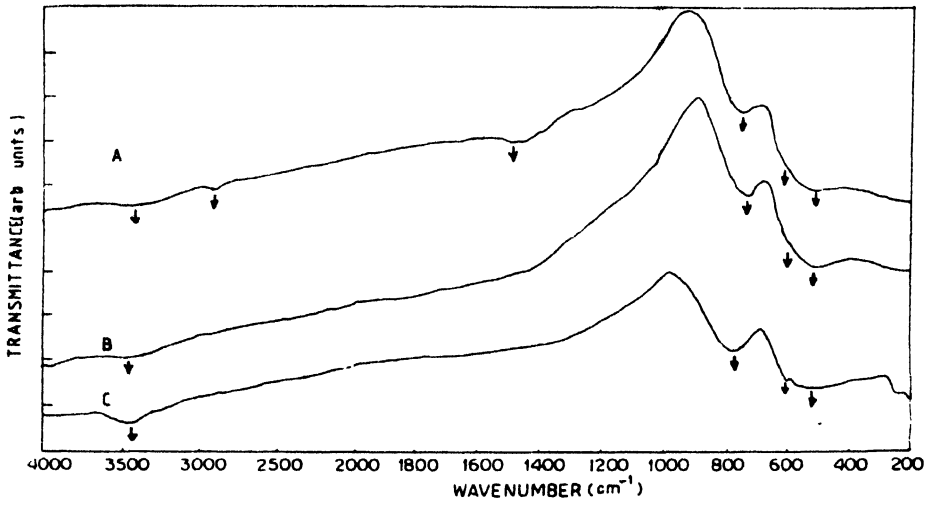

Figure 8. IR spectra of ($Bi_4Sr_3Ca_3Cu_yO_x$) glasses (A : y = 3, B : y = 4, C : y = 5)

It is well known [58] that the Bi-Ca-Sr-Cu-O oxide systems contains a number of superconducting phases in the series $[Bi_2Ca_{n-1}Sr_2Cu_nO_{2n+4}]$. Three well known superconducting phases viz. $[Bi_2Ca_1Sr_2Cu_1O_6]$, $[Bi_2Ca_1Sr_2Cu_2O_8]$, and $[Bi_2Ca_2Sr_2Cu_3O_{10}]$ have T_c value between 84-110K. The superconducting phases obtained by annealing a glass phase contains, in most cases, both high T_c and low T_c phases. It is rather difficult to obtain a single phase superconductor unless prolonged annealing of the glass sample is carried out. The gradual appearence of cystalline phases and hence superconducting peaks with the increase of annealing time is shown in the X–ray diffraction pattern (Figure 9) and also in the SEM photos (Figure 10). Elaborate microstructural studies of the $Y_1Ba_2Cu_3O_x$ (1:2:3) glasses have been carried out by Murakami *et al* [20]. They showed the possibility of increasing J_c value of the corresponding superconducting phase.

Though the actual crystallization processes in these Bi or Y–based glasses are yet to be understood, it appears that the low T_c phase or impurity phases nucleate first and gradually grow depending on the annealing time and temperature. Recently Shi *et al* [26, 59] attempted to study the crystallization of glassy oxides (2:2:2:3), (2:2:3:4), and (2:2:4:5) on the basis of nucleation theory. The presence of impurity phase like $CuCa_2O_3$, CaO etc. appearing during low temperature annealing (500°C) gradually disappears or greatly reduced during high temperature (~800°C) long time annealing [26, 27, 59-61].

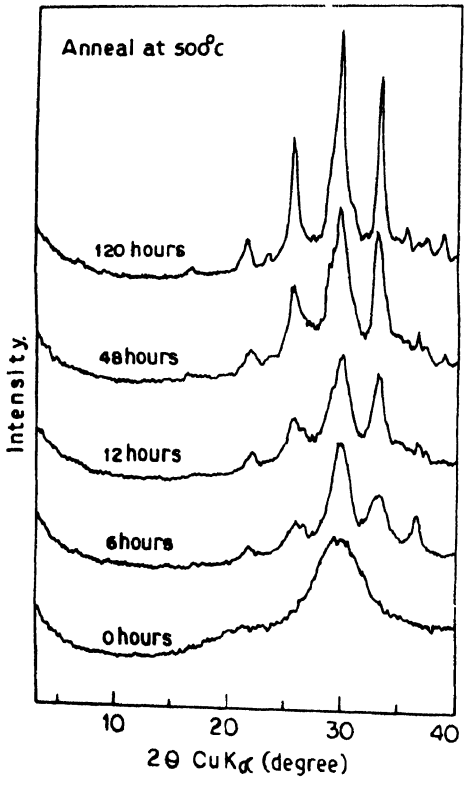

Figure 9. Changes in the X-ray diffraction patterns depending on annealing time [60].

An estimate of the absolute theoretical volume of a superconducting phase in the sample can be calculated from [53] as

$$V = \frac{V_{sc}}{V_{san}} = \frac{E/C}{\overline{W}/\rho_d} \times 100\ (\%) \tag{5}$$

where E is an inductance change (dB), C is an equipment constant (21 dB/cm^3), $\overline{W}$ is the sample weight (g), and ρ_d is a theoretical density of the sample (g/cm^3). Figure 11 shows

the volume ratio of superconducting phase calculated from eq. (5) in the glass samples ($BiSrCaCu_2O_x$ [53]) annealed at various temperatures. The volume ratio shows a maximum

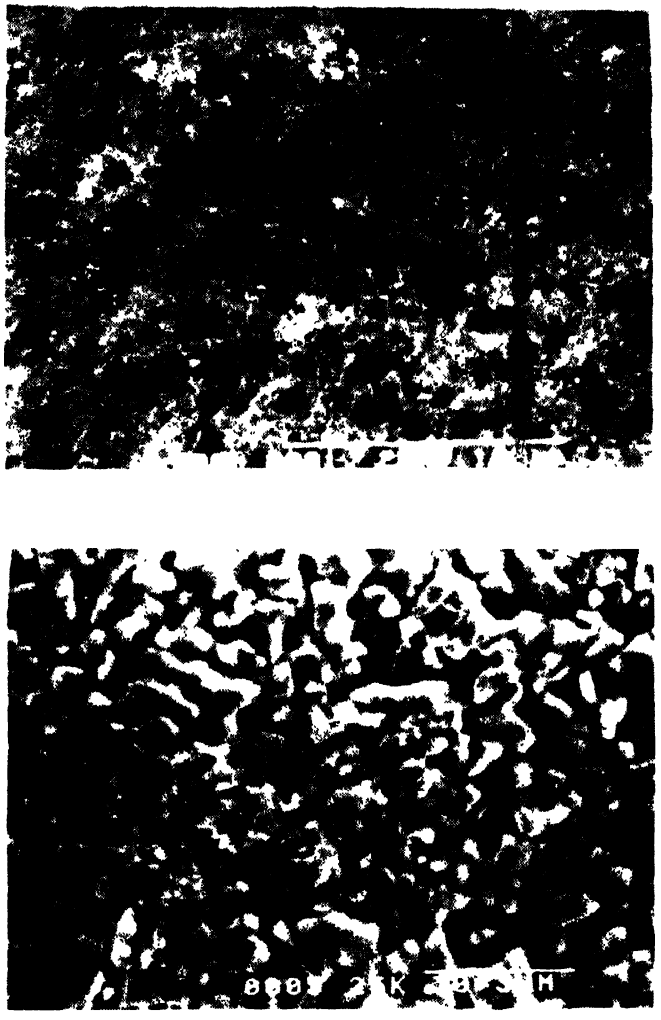

Figure 10. Scanning electron micrographs of the same sample shown in Figure 3, after annealing at 700°C for 3 h (a), and at 820°C for 28 hours (b). This sample (b) is superconducting with T_c ~85K [23].

value of 70-75% ($BiSrCaCu_2O_x$ glass), 85-90% (for $Bi_4Ca_3Sr_3Cu_4$ glass) for annealing the samples between 800-850°C. Therefore, it appears that there is a 'critical' annealing time and temperature for all these Bi- or Y- based oxide glasses for obtaining maximum volume % of superconducting phases. Above and below this critical annealing temperature this volume ratio decreases. The X–ray diffraction studies [49] also supports this contention that the impurity phases are reduced if the sample is heated at a proper annealing temperature for an appropriate time. Annealing above 850°C, the glasses melt and superconducting volumes

decrease due to decomposition of superconducting phases into the corresponding semiconducting phases. Stable superconducting phases are obtained only in a limited

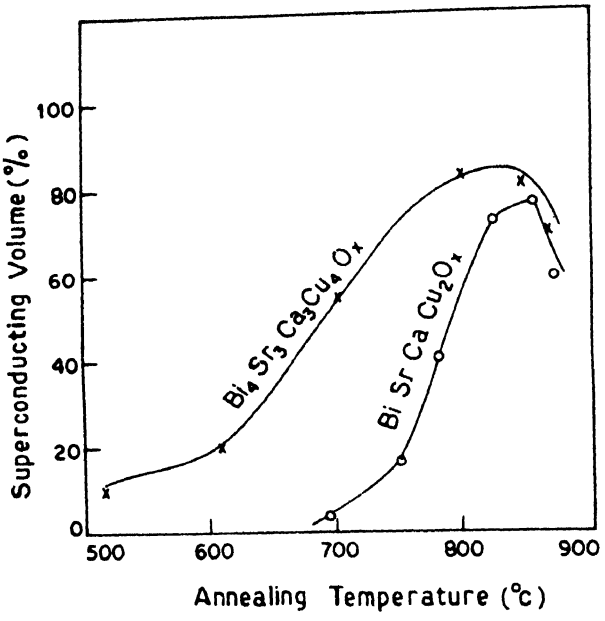

Figure 11. Volume ratio of superconducting phase of $BiSrCaCu_2O_x$ [53] and $Bi_4Sr_3Ca_3Cu_4O_x$ glasses.

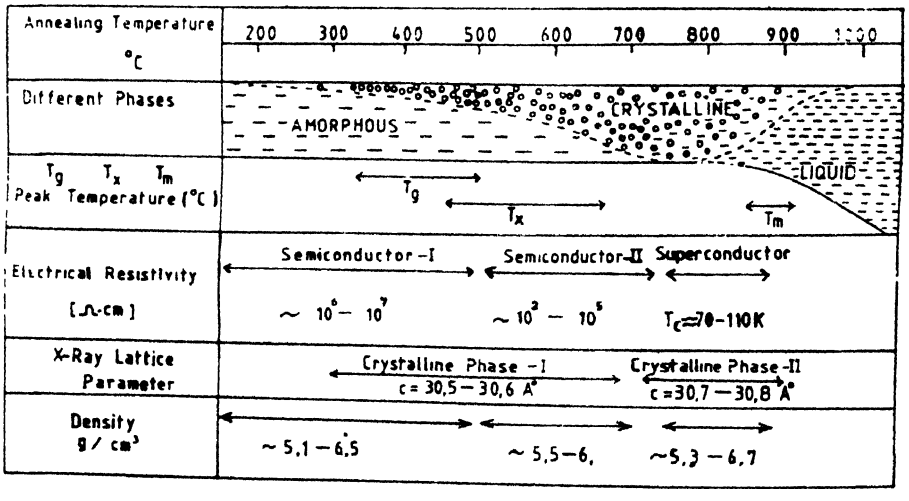

Figure 12. Schematic behaviour of the glasses and ceramic superconductors depending on annealing time and temperature.

temperature range. In Figure 12 we have summarized the X-ray, DTA, and some other behaviour of the glasses, in general, depending on the annealing temperature. The reason

why the total superconducting volume ratio decreases above a critical temperature of annealing (say 840°C for the (1:1:1:2) system) might be, as suggested by Kanai *et al* [53], due to the decomposition of the low T_c superconducting phase into two components, one superconductor and the other non-superconductor.

The chemical changes occurring due to low temperature annealing can be expressed as

$$[Bi_2(Sr, Ca)_2CuO_x]_{glass} \xrightarrow[500\text{-}800°C]{12h} [Bi_2(Sr, Ca)_2CuO_x]_{sc}$$

$$[Bi_2(Sr, Ca)_2CuO_x]_{glass} + (Sr, Ca)CuO_2 \xrightarrow[600\text{-}800°C]{12h} [Bi_2(Sr, Ca)_3Cu_2O_y]_{sc}$$

and

$$[Bi_2(Sr, Ca)_2CuO_x]_{sc} + (Sr, Ca)CuO_2 \xrightarrow[600\text{-}800°C]{12h} [Bi_2(Sr, Ca)_3Cu_2O_y]_{sc}$$

Takei *et al* [60] showed from XRD and SEM and SEM-EPMA data that a glass specimen annealed at 500°C is in an intermediate state between glassy and crystalline phases. Diffraction peaks appear sharper with an increase in the annealing time. The XRD patterns [60] of the glass powder annealed at 500°C for 120h are much broader than those of the samples annealed at 600°C for 12 hours. Therefore proper choice of the annealing time and temperature depending on the glass compositions are very important for crystallization of the glasses to their corresponding superconducting phases. It is however, noticed that prolonged annealing of the glass samples (below the corresponding melting point by about 50°C) give better quality superconducting materials from the glasses. In Table 2 we have shown the variations of superconducting transition temperatures with annealing time and temperatures for some glasses of our interest.

Table 2. Annealing temperature, time of some glass smaples and the corresponding superconducting transition temperatures (all the samples are air annealed and slowly cooled).

Glass Samples	Annealing temperatures (°C)	Annealing time	T_{co} (K)
$Y_1Ba_2Cu_3O_x$	900	15 min	—
	950	30 min	45±3
	930	24 h	90±5
$Bi_4Sr_3Ca_3Cu_4O_x$	850	15 min	50±2
	850	2 h	60±2
	850	2 days	85±2
	865	12 h	95±10
$Bi_{1.5}Pb_{0.5}Sr_2Ca_2Cu_3O_x$	500	12 h	—
	720	24 h	75±5
	800	24 h	70±5
	840	10 days	10±5
	850	3 days	98±5
	850	4 days	68±5

The crystallization processes of many of these glasses are, however, very complicated. From classical nucleation theory the nucleation rate N_r is given [62]

$$N_r \alpha n\upsilon \exp\left[\frac{-\Delta G_c}{k_B T}\right] \exp\left[\frac{-E_a}{k_B T}\right] \quad (6)$$

where n is the number of atoms per unit volume, υ = oscillating frequency of the atoms, G_c is the free energy required to form a nucleus of a critical size r, and E_a is the activation energy for a crystal growth.

5. Properties of some ceramics and glasses

5.1. Superconducting ceramics (annealed glasses) :

It should be mentioned at this point that the superconducting behaviour of the ceramics obtained from their corresponding glass phases are almost similar [63] to those superconducting oxides obtained from (SSR) technique. So elaborate discussion on the properties of the superconductors obtained from the (GCR) technique has not been made which may, however, be obtained from the standard published literature [63]. Some of the chatracterstic parameters of these superconductors have already been shown in Table 1 (A, B, and C). There are mainly three types of superconducting oxide glasses from which HITSO materials have been prepared by annealing viz. (Y–Ba–Cu–O), (Bi–Sr–Ca–Cu–O), and (Bi–Pb–Sr–Ca–Cu–O) systems. The superconducting properties (like thermal variations of electrical resistivity, magnetic susceptibility (both ac and dc), critical current density (J_c) etc. of these superconductors largely depend on the composition of the glasses, annealing time and annealing process, cooling rate of the sample etc. For the Bi– based glasses T_c values do not depend appreciably on the atomspheric conditions of the furnace where the glass samples are annealed: The general behaviour of the superconductors obtained from the glass phase and those obtained by usual (SSR) technique (i.e. by heating the powders) are almost the same. We are discussing below some of the properties of the different superconductors obtained from the glasses.

(i) Y–Ba–Cu–O system :

The $YBa_2Cu_3O_x$ (1:2:3) glasses were first obtained by Komatsu *et al* [18]. Though (1:2:3) glasses are rather difficult to make requiring higher quenching rate than that required for the Bi–based glasses, very high quality (high J_c and T_c values [20]) superconducting films and bulk materials can be prepared from this glass [20]. Some resistivity and ac magnetic susceptibility curves of this superconductors as a function of temperature are shown in Figure 13. Very good quality films having high J_c value (J_c = 7400 A/cm^2 at 77K) have also been prepared from this glass [20].

(ii) Bi–Sr–Ca–Cu–O system :

This system has been vastly studied both in the glassy as well as in their corresponding superconducting phases (see Table 1B). In the $Bi_2Sr_2Ca_{n-1}Cu_nO_x$ (n=1,2,3) series,

$Bi_2Sr_2CuO_x$ (with T_c = 10K), $Bi_2Sr_2CaCu_2O_x$ (with T_c =80K) and the $Bi_2Sr_2Ca_2Cu_3O_x$ (with T_c ≒105K) systems have been well studied. Another very interesting glass of this series

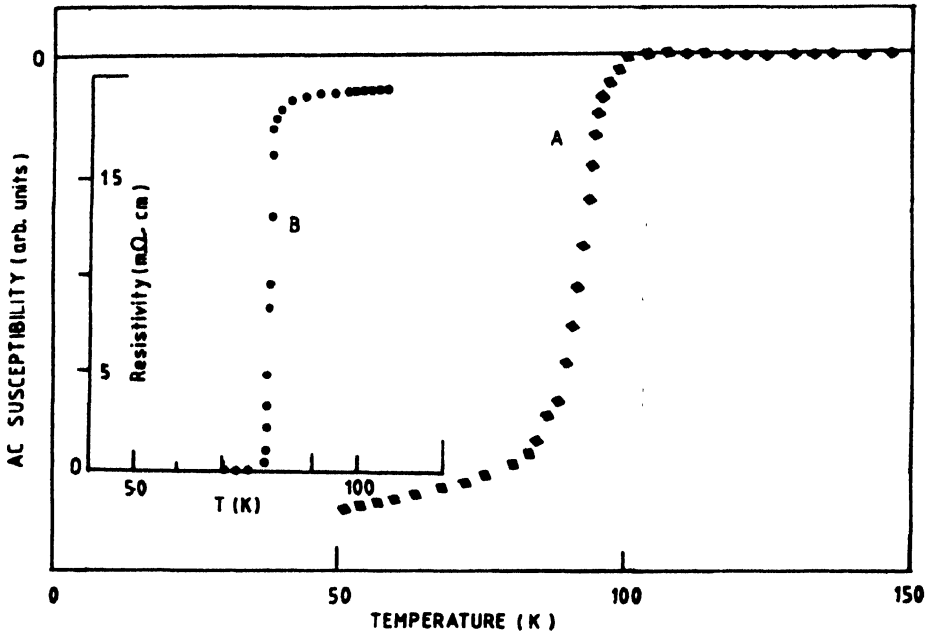

Figure 13. Electrical resistivity (B), and ac susceptibility (A) of a typical $Y_1Ba_2Cu_3O_x$ superconductor obtained from the glass phase.

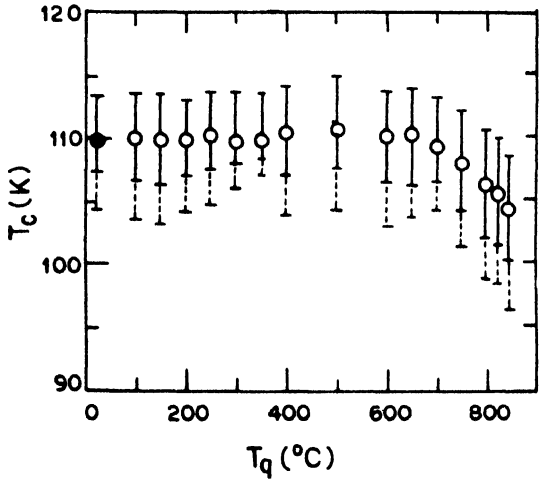

Figure 14. Variation of T_c with quenching temperature of a typical $Bi_{0.96}Pb_{0.24}SrCaCu_{1.6}O_x$ glass system [68].

viz., $Bi_4Sr_3Ca_3Cu_4O_x$ with relatively low T_c (= 85K) is found to be very suitable for making superconductor from the glassy phase. Shi *et al* [26, 59] reported T_c above 100K for

the (2:2:3:4) and (2:2:4:5) systems. Although some authors reported T_c < 70K for the (2:2:1:2) system obtained from the corresponding glass phase (Table 1B), the T_c values of the (2:2:2:3) superconductor was reported to be between 80-86K. This large variation of T_c with small change of Cu concentration is interesting. The dependence of T_c on the annealing conditions of the (1.2:1:1:2) and (2:2:1:2) systems have also been reported by Komatsu *et al* [24]. The variation of T_c with quenching temperature is shown in Figure 14. The corresponding variation of resistivity of the same ceramic superconductor depending on quenching temperture is shown in Figure 15. The dependence of T_c on the oxygen content of the Bi-based superconductor obtained by GCR method has not yet been reported.

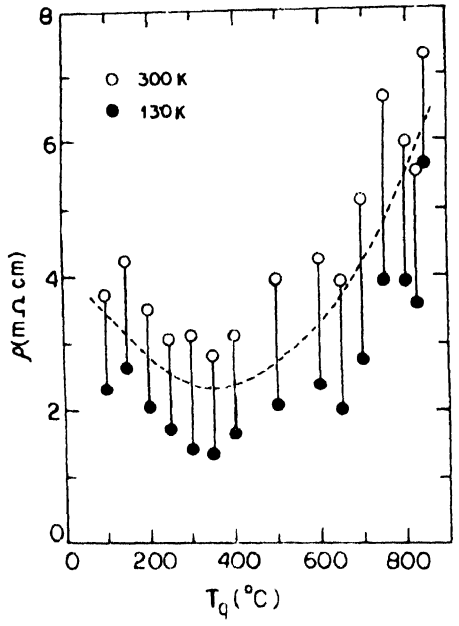

Figure 15. The variation of resistivity of the $Bi_{0.96}Pb_{0.24}SrCaCu_{1.6}O_x$ glass with quenching temperature [68].

Many Bi-based low T_c (75-85K) prolonged annealed superconductors indicate small anomalies at about 105K due to the presence of higher T_c phase in those systems [24]. However, it should be pointed out that appropriate choice of the glass composition is necessary for obtaining this high T_c phase from its glass phase. In general, for all low temperature (below 700°C) and long time annealed samples, the room temperature resistivities are higher than those of the high temperature long time annealed samples. The long time and high temperature (above 800°C and below melting) annealed samples are very good superconductors obtained by (GCR) method.

The temperature variation of ac magnetic susceptibility of some Bi-based superconductors annealed at different temperatures are shown in Figure 16. It is observed

from this figure that the onset temperature decreases with decrease of annealing temperature for the (2:2:1:2) superconductor. This behaviour is consistent with behaviour of resistivity

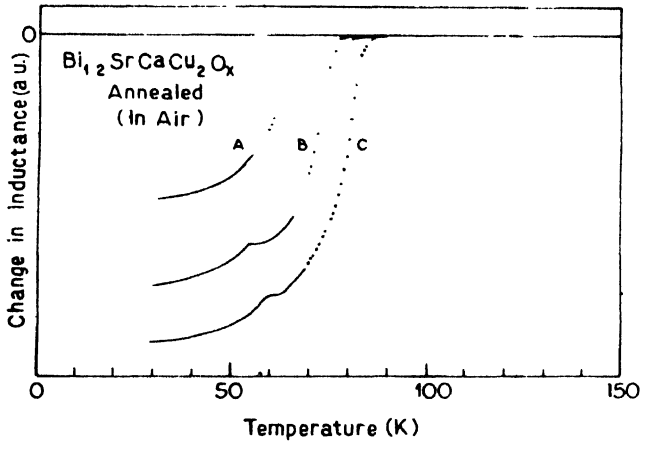

Figure 16. Temperature dependent ac magnetic susceptibility of a furnace cooled Bi-based superconductor obtained from its glass phase (A - 760°C, 20h ; B : 800°C, 20h ; C : 850°C, 20h) [24].

(Figure 15) and is associated with the degree of crystallinity, purity of the superconducting phase (single or multiphase) which increases with the increase of annealing time and temperature (below melting) etc. Compared to the (1.2:1:1:2) glass the (2:2:1:2) glass produces better superconductor. The J_c values of the different Bi-based oxide superconductors obtained from the glassy phases are found to vary between 30-50 A/cm^2 at 77K [24] which is comparable to those of the superconductors obtained from the pure ceramic or chemical routes. Actually the presence of non-superconducting phases like CuO, and some ions like Cu^{2+}, Bi^{3+}, Ca^{2+} etc. at the grain boundaries as well as random orientation of the superconducting crystallites which enhances weak coupling at the grain boundaries reduce both T_c and J_c values and also broadens the $(T_c - T_{co})$ region. This is also responsible for showing anomalies or kink in the resistivity and magnetic susceptibility curves as a function of temperature [24, 64]. In many cases such anomalies in the superonductors obtained from the glass phases could be removed by making homogeneous glass and by controlling the annealing time and temperature.

Heat treatment of the different glasses in oxygen, nitrogen, argon or air did not affect very much the superconducting behaviour of the systems. One interesting behaviour is, however, observed by us that the superconductors obtained by annealing the glass in oxygen atmosphere gives better electrical resistivity versus temperature curve whereas the same glass annealed in air gives better magnetic susceptibility versus temperature curve (i.e. $T_c \approx T_{co}$). Another intersting behaviour is that the same glass annealed at different temperatures for different times might behave as semiconductor or superconductor [27, 65].

The T_c for the (1.5:1:1:2) sample was found to be highest (104K) with T_{co} = 100K. For (1.2:1:1:2) sample Komatsu *et al* [24] obtained T_c = 75K. This might be due to the effect of increase of Bi_2O_3 concentration. However, elaborate investigation of the effect of the change of Bi in the glass on T_c has not yet been investigated except for the (4:3:3:4) glass [52, 66]. The electrical resistivities and dc magnetic susceptibilities [52, 65] of some (4;3:3:y) type superconductors and glasses are shown in Figures 17 and 18 respectively.

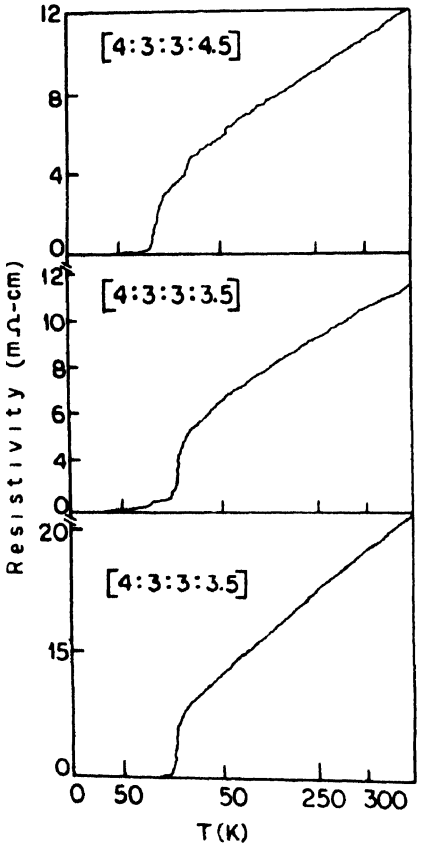

Figure 17. Variations of the electrical resistivities of the ($Bi_4Sr_3Ca_3Cu_yO_x$) type superconductors on the CuO concentrations.

Hinks *et al* [54] reported the presence of two superconducting phase in the (2:2:2:3) composition with T_c = 110K and T_c = 85K (low T_c phase). The (1:1:1:2) glass prepared by Komatsu *et al* [34] with low Bi concentration was, however, found to have high T_c = 102K (T_{co} = 92K) value with high J_c = 102 A/cm^2 at 77K and zero field. This sample was annealed at 800°C for 24 hours in O_2. They also obtained superconductivity in this sample annealed at 300°C for 28 hours in presence of oxygen. The rapidly cooled glass samples, in general, show high T_c and sharp superconducting transition. However, slow furnace cooled sample after annealing might show low T_c and broad transition with a tail.

The (2:2:1:2) superconducting film produced by GCR [31] was found to have T_c = 86.8K. Thin film of 20 μm thick was made by twin roller technique at a cooling rate of 10^5K/Sec. Thick films and wires with (4:3:3:4) glass were also prepared [23, 66] and found to have T_c = 84K with J_c = 200 A/cm^2.

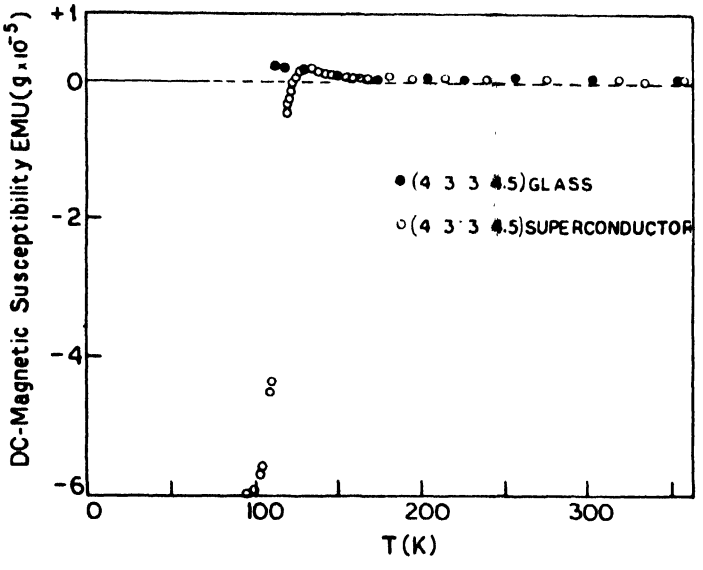

Figure 18. Temperature dependence of dc magnetic susceptibilities of a typical (4 : 3 : 3 : 4) glass and superconductor.

(iii) Bi–Pb–Sr–Ca–Cu–O systems :

Another very interesting oxide superconductor viz. Bi–Pb–Sr–Ca–Cu–O system has also been prepared from its glass phase [32, 64, 68, 69]. The addition of PbO appears to produce mostly single phase Bi–Sr–Ca–Cu–O glass. This glass with different concentrations of Pb or Bi were prepared from Bi_2O_3, $SrCO_3$, $CaCO_3$, CuO and PbO. Ibara *et al* [32] prepared $BiPb_ySrCaCu_2O_x$ (y = 0.1, 0.2, 0.3 and 0.4) having T_c = 120K and T_{co} = 102K (for the y = 0.1 sample). Ishida [68] also reported T_c = 110K in the $Bi_{0.94}Pb_{0.24}SrCaCu_{1.6}O_x$ system. Komatsu *et al* [34] studied $Bi_{0.8}Pb_{0.2}SrCaCu_{1.5}O_x$ showing T_c = 100K in the superconducting phase obtained by prolonged annealing in air for 250h at 840°C. The critical current density J_c at 77K and zero magnetic field was reported to be 120 A/cm^2. It is observed for the Pb containing glasses that for the higher values of the glass transition temperature T_g, the superconducting transition of the corresponding sample (annealed) is lower. For example, $Bi_{0.96}Pb_{0.24}SrCaCu_1O_x$ glass has T_c = 650°C with T_c = 110K and the $BiPb_{0.1-0.4}SrCaCu_2O_x$ glass T_c lies within 480°C having maximum T_c = 122K. This contention appears to be true for all the glasses becoming superconducting after annealing. Furthermore, the superconducting behaviour of the Bi–Sr–Ca–Cu–O and the Bi–Pb–Sr–Ca–Cu–O sysyems unlike the Y–Ba–Cu–O system do not depend on the furnace atmosphere,

whether air, oxygen, or some other glasses. Addition of Pb also increases the volume fraction as well as stability of the high T_c phase in the Bi–based systems [32, 64, 68, 69].

Finally it should be mentioned here that the Tl–Ba–Ca–Cu–O system has not been prepared from the glass phase. However, this system has also been obtained from the semi glass-ceramic route [70]. Here the Ba–Ca–Cu–O system was first melted by heating appropriate amount of the oxides at 1100°C for about three hours. The solid glass is made by quick quenching this melt in between two copper blocks. The thin glass plates thus prepared are annealed at 800°C for about 24 hours. This annealed plate is sealed inside quartz or silver tube with appropriate amount of Tl_2O_3 which is then heated inside the furnace at about 900°C for 10 to 20 minutes (depending on the thickness of the plates). The furnace is then cooled slowly. The sample inside the silver tube is found to be superconducting with T_c around 120K. This is a mixed phase superconductor. The electrical resistivity and ac magnetic susceptibility of this superconducting thick film are shown in Figure 19. This might be a good technique for making Tl– based high T_c superconducting dense films.

Some reports on the preparation of metallic Bi–Sr–Ca–Cu alloys from melt and then converting them to the corresponding superconducting phase [71] have also been made.

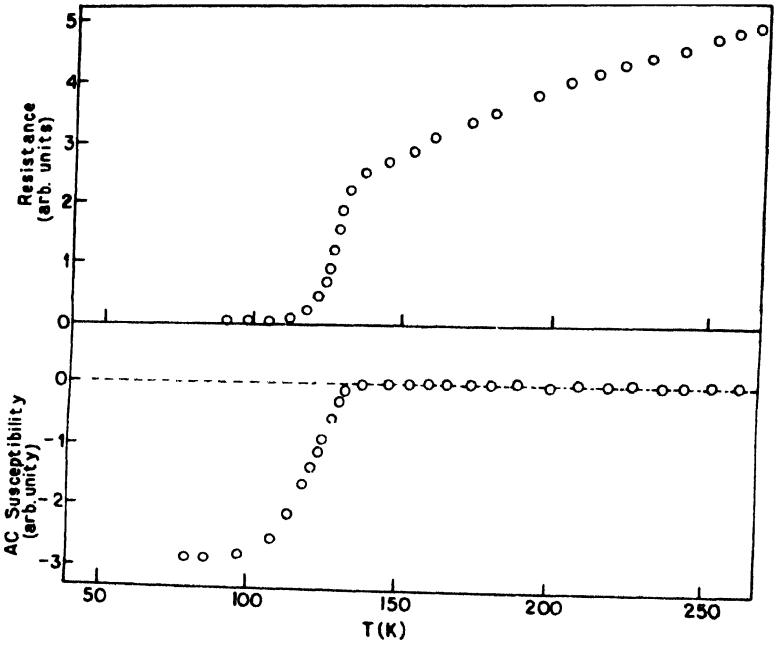

Figure 19. Thermal variations of electrical resistivity and ac susceptibility of a $(Tl_2Ba_2Ca_1Cu_2O_x)$ type superconductor thick film obtained from semi-glass-ceramic route.

It should be pointed out further that the method of converting the glass phases to their corresponding superconducting phase is a tricky one. Often good superconductors from the glasses are found when the glass is made with about 1% of silver in it or by annealing

the glass samples in a silver container or tube. Probably the presence of silver helps attaining the correct oxygen content in samples. This was also pointed out by Baker *et al* [72].

5.2. Properties of glasses which become superconductor by annealing :

For a better understanding of the mechanism of superconductivity of the annealed glasses (Bi, or Y–based), a critical analysis of their electrical, magnetic, optical, and other properties are necessary. However, very little investigation of the electrical, dielectric or other properties of these glasses have so far been made [23-27, 48, 67, 73]. We shall discuss below the semiconducting properties of some of these glasses (non-superconducting samples) like $Bi_4Sr_3Ca_3Cu_yO_x$ (y = 3.5, 4, 4.5, and 5) which are homogeneous and single phase in character. If the glass sample like $Bi_4Ca_3Sr_3Cu_4O_x$, $Bi_{1.5}SrCa_3Cu_3O_x$, $Bi_{1.5}SrCaCu_2O_x$ etc. are heat treated at 200°C for 2 hours in O_2, N_2, or Ar, no change in the electrical properties are observed [25]. Though no report of the existence of superconducting phase in the homogeneous glass sample has been observed down to 4.2K, Varma *et al* [50] concluded from non-resonant microwave absorption (at 9.1 GHz) that the weak microwave absorption at 77K in a (Bi–Ca–Sr–Cu–O) glass is due to the existence of clusters or ultra microcrystallites of superconducting phase in the glass. More elaborate investigations to confirm the existence of superconducting phase even in the glass would be interesting. This might help to understand the origin why these very oxide glasses become superconducting when annealed. Of course, such microcrystalline regions in some inorganic glasses have already been observed by Krivanek *et al* [74].

The (SEM) micrograph of a typical (4:3:3:4) glass after annealing at 250, 400, 700 and 830°C, respectively, for 2, 3, 4, and 15 hours are shown in Figure 3. The heat treated micrographs show an indication of phase separation after heat treatment which disappears by heat treatment at higher temperature and for a longer time. Similar indication of phase separation was also noticed from the CuO concentration variation of density and apparent molar volume of oxygen V^* as discussed in Section 3.2. Although the separated phase composition has not yet been determined, ac electrical conductivity results and Cu_2O crystallization detected by X–ray diffraction after switching [57] suggested that this phase could be mostly the precipitated Cu_2O. All the glass samples with the variations of CuO concentrations in the ($Bi_4Sr_3Ca_3Cu_yO_x$, y = 5, 4.5, 4, 3.5, 3) did not show phase separation (for example (4:3:3:5), and (4:3:3:4) though some very small isolated and dispersed crystallites appear. They are mostly precipitate of CuO since these glasses have a very high concentrations of CuO.

An ohmic behaviour upto 300V is observed above which a non-linear electric field effect of a Poole-Frenkel (electronic) mechanism is considered to be valid. The straight line region of the I-V curve can be fitted with

$$\log I = \beta V^2 \tag{7}$$

where β is the decay coefficient of the applied electric field [16].

6. Electrical properties of Bi-Sr-Ca-Cu-O glass

6.1. DC conductivity of the glasses :

Detailed electrical conductivity of the (4:3:3:4) type glasses have only been studied so far [48, 59, 66]. In the temperature range of 77-450K these glasses show interesting semiconducting behaviour. The values of dc conductivity (σ_{dc}) of these glasses at a fixed temperature (300K) is shown in Figure 20. It is observed that (σ_{dc}) increases with the increase of CuO concentrations. The activation energy (W) of the glasses, however, decreases with increase of CuO content in the glass (Figure 20). It is interesting to mention that though these glasses become superconductors after annealing, the room temperature conductivities of these glasses are about two order of magnitudes lower those of the V_2O_5 or Fe_2O_3 containing TMI glasses [11, 12, 76]. It may be noted that the magnitudes of (σ_{dc}) of the (4:3:3:y) glasses at any temperature tends to be higher in those glasses having lowest thermal activation energy. These results, however, agree with those for the vanadate type glasses [11, 12]. It is also noted that at 300K the activation energy of the (4:3:3:y) glasses is higher than that of the V_2O_5–Bi_2O_3, or Fe_2O_3–Bi_2O_3 glasses. The thermopower measurements at room temperature shows that the charge carriers are mostly electrons.

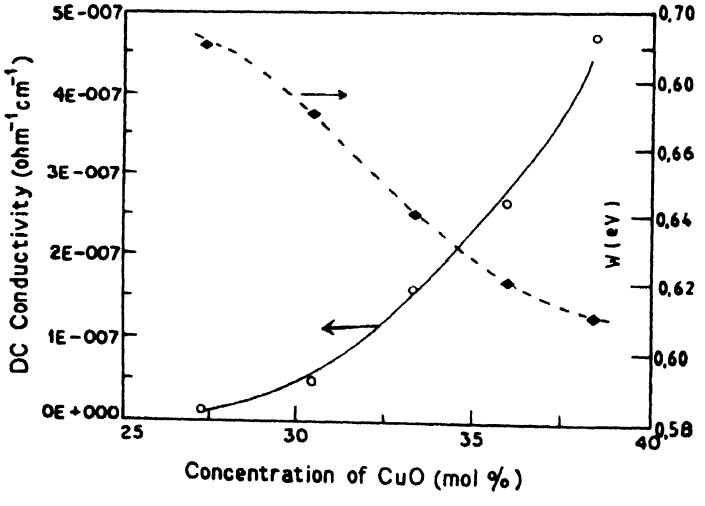

Figure 20. DC conductivities (σ_{dc}) and activation energeis (W) of a Bi-based glass as a function of CuO concentrations.

The logarithm of measured dc conductivity (σ_{dc}) of the (4:3:3:y) glasses as a function of inverse temperature is shown in Figure 21. The slopes of the curves change with temperature indicating temperature dependent activation energy (W). This is a characteristic feature of hopping conductivity in these glasses similar to those observed in many other (TMI) glasses [1–16]. The activation energy of the glasses decrease slowly below 280-300K and at the lowest temperature region (77K) it becomes ≈ 0.05eV. This behaviour is

consistent with the polaron model of hopping conduction [6] which predicts an appreciable departure from a linear T^{-1} versus log σ_{dc} plot below a temperature $T_t < \theta_D/2$ (θ_D is the Debye temperature). From the analysis of the dc conductivity data as a function of Cu-concentration (Figure 20) and temperature (Figure 21), one finds that the observed

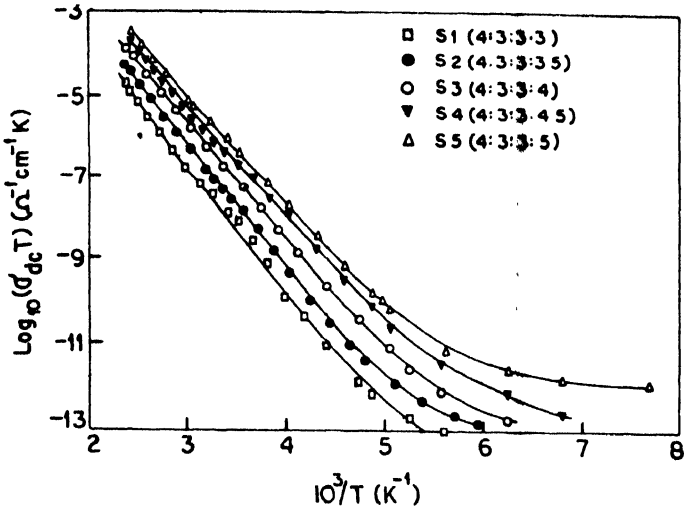

Figure 21. Variation of log σ_{dc} with $\frac{1}{T}$ of the Bi-based glasses.

dependences are well discussed by Mott's theory [5, 6] which regards the electrical conductivity of the semiconducting oxide glasses as a process similar to the impurity conduction in doped and compensated semiconductors. According to this theory, the expression for dc electrical conductivity is written as

$$\sigma_{dc} = \sigma_o \exp \frac{-W}{K_B T} \tag{8}$$

where the factor σ_o is dependent on the distances between ions (TMI) and may be written as

$$\sigma_o = \frac{\upsilon_{ph} e^2}{k_B T k} C(1-C) \exp(-2\alpha R) \tag{9}$$

where υ_{ph} is the optical phonon frequency, R the average site spacing which is estimated from the relation $R = \left(\frac{1}{N}\right)^{\frac{1}{3}}$ (N being the number of copper sites per unit volume), C is the ratio of the TMI ion concentration in the low valency state to the total TMI ion concentrations, α is the wave function decay constant, k_B is the Boltzmann constant. For a typical (4:3:3:4) glass the model parameters [51, 66] fitted with eq. (9) are shown in Tables 3-5.

If W_H is the polaron hopping energy and W_D is the disorder energy arising from the energy difference of the neighbouring sites, the activation energy W is given by

$$W = W_H + \frac{W_D}{2} \quad \text{for} \quad T > \frac{\theta_D}{2} \tag{10}$$

$$= W_t \qquad \text{for} \quad T < \frac{\theta_D}{4}$$

The Debye temperature $\theta_D = \frac{h\upsilon_{ph}}{k_B}$ (h is the Planck's constant). From the results of chemical analysis and the density of the glasses, the mean distance R between the copper ions has been calculated (see Table 3). The variation of R with $\log \frac{\sigma_o}{C(1-C)}$ is shown in Figure 22. Since each composition of the glasses differs by the $\frac{Cu^{+1}}{Cu_{total}} = C$, σ_o is divided by the factor $C(1-C)$. From the slope of Figure 22 the value of α is calculated. These values of α as shown in Table 5 indicate strong localized states in the (4:3:3:y) type glasses [48].

Table 3. Some characteristic parameters of $(Bi_4Sr_3Ca_3Cu_yO_x)$ (4:3:3:y)* type glasses for different values of CuO concentrations.

Sample	G1	G2	G3	G4	G5	G6	G7	G8
Composition (Cu content y)	0	1	2	3	3.5	4	4.5	5
Starting Cu content (wt%)	0	4.26	8.09	11.56	13.17	14.70	16.17	17.57
Final Cu content (wt%)†	0	4.63	8.21	11.64	14.05	15.90	17.22	18.08
Mole % of CuO	0	11.11	20.00	27.27	30.43	33.33	36.00	38.46
Density (ρ) (gm/cm^3)	5.969	5.954	5.932	5.921	5.892	5.890	5.876	5.859
N ($10^{21} eV^{-1} cm^{-3}$)	—	2.61	4.61	6.53	7.84	8.87	9.59	10.04
$C = Cu^+/Cu_{tot}$	—	0.79	0.75	0.70	0.75	0.78	0.80	0.79
R (Å)	—	7.261	6.007	5.350	5.033	4.831	4.707	4.635
r_p (Å)	—	2.926	2.421	2.156	2.028	1.947	1.897	1.868
T_g (°C)	480	402	422	422	440	426	446	431
T_x (°C)	505	512	534	495	555	532	532	491
$(T_x - T_g)$ (°C)	97	110	112	73	115	106	86	60

* All these glasses are found to be superconducting with T_c varying from 85 to 100K [51]

† From chemical analysis and atomic absorption spectorscopy.

Table 4. Some characteristic parameters of the $(Bi_4Sr_3Ca_3Cu_yO_x)$ glasses obtained by fitting the experimental conductivity data with different theoretical models.

Sample	σ_{dc} (ohm^{-1} cm^{-1})		W (eV)		W_H[a] (eV)	ΔW (eV) $= W - W_H$	W_D (eV)
	at 300K	at 410 K	300K	410K			
G2	1.03×10^{-12}	8.70×10^{-10}	0.660	0.820	0.18	0.480	0.062
G3	2.42×10^{-12}	1.50×10^{-9}	0.634	0.760	0.22	0.414	0.043
G4	9.00×10^{-11}	2.53×10^{-8}	0.580	0.709	0.25	0.330	0.050
G5	2.05×10^{-10}	4.71×10^{-8}	0.568	0.684	0.26	0.308	0.030
G6	7.70×10^{-10}	2.31×10^{-7}	0.544	0.656	0.28	0.264	0.029
G7	1.70×10^{-9}	3.80×10^{-7}	0.526	0.637	0.28	0.246	0.037
G8	3.90×10^{-9}	6.95×10^{-7}	0.510	0.625	0.29	0.220	0.029

a) Calculated from eq. (13) assuming $\varepsilon_p = \varepsilon_\infty = n^2$ (where n = 1.995)

Table 5. Some characteristic model parameters obtained from the electrical conductivity data characterizing the behaviour of the ($Bi_4Sr_3Ca_3Cu_yO_x$) glasses.

Sample	$\vartheta_{ph}\exp(-2\alpha R)$ (Hz)	$\vartheta_{ph}^{a)}$ (Hz)	$\alpha^{b)}$ ($Å^{-1}$)	$\alpha^{c)}$ ($Å^{-1}$)	$\gamma_p \approx 2W_H/\hbar\omega_0$	$m_p/m_e = \exp(\gamma)$
G2	2.92×10^{9}	1.34×10^{13}	0.47	0.98	8.69	5.9×10^{3}
G3	4.00×10^{9}	1.25×10^{13}	0.46	0.92	10.62	4.1×10^{4}
G4	7.78×10^{9}	1.01×10^{13}	0.45	1.23	12.07	1.7×10^{5}
G5	1.13×10^{10}	9.5×10^{12}	0.45	0.99	12.56	2.8×10^{5}
G6	1.38×10^{10}	8.88×10^{12}	0.44	0.97	13.52	7.5×10^{5}
G7	1.64×10^{10}	8.94×10^{12}	0.44	0.75	13.52	7.5×10^{5}
G8	1.69×10^{10}	8.40×10^{12}	0.44	0.87	14.00	1.2×10^{6}

a) Calculated from the values of $\vartheta_{ph}\exp(-2\alpha R)$ assuming $\alpha = 0.669 Å^{-1}$ as obtained from the slope of R vs $\log\left[\frac{\sigma_0}{C(1-C)}\right]$ curve (Figure 22)

b) Calculated from the values of $\vartheta_{ph}\exp(-2\alpha R)$ assuming $\vartheta_{ph} = 10^{13}$ Hz

c) Calculated from the slope of $T^{-1/4}$ vs. $\log\left(\sigma_{dc} T^{1/2}\right)$ curve (figure 25)

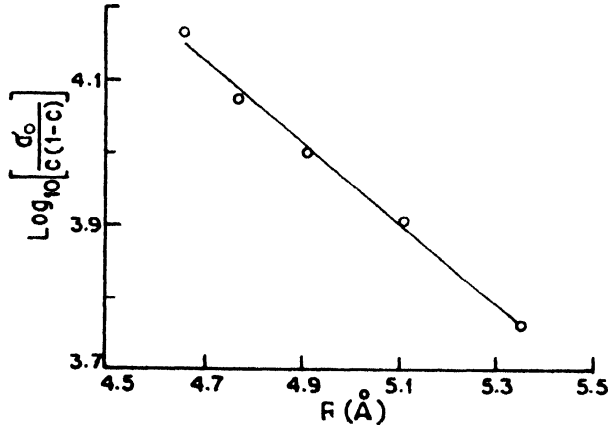

Figure 22. Variation of R with $\log\left[\frac{\sigma_0}{C(1-C)}\right]$ of the Bi-based (4 : 3 : 3 : y) glasses with y = 3, 3.5, 4, 4.5, 5.

An attempt has also been made to calculate the optical phonon frequency for the glasses by fitting the log σ versus $\frac{1}{T}$ curves (Figure 21) with the Holstein's [77] relation viz.

$$\sigma = \frac{Ne^2R^2J^2}{2\hbar\omega k_BT}\left[\frac{\pi}{Wk_BT} \times \frac{\sinh\frac{\hbar\omega_0}{2k_BT}}{\frac{\hbar\omega_0}{2k_BT}}\right]^{\frac{1}{2}} \exp\left(-\frac{W_D + GW_P}{2k_BT}\right) \qquad (11)$$

where $G = \dfrac{\tanh \dfrac{\hbar\omega_o}{2k_BT}}{\dfrac{\hbar\omega_o}{2k_BT}}$, the polaron bandwidth J should satisfy the inequality

$$J > \left(\frac{2k_BTW_H}{\pi}\right)^{\frac{1}{4}} \left(\frac{h\upsilon_{ph}}{\pi}\right)^{\frac{1}{2}} \quad \text{for adiabatic hopping}$$

$$< \left(\frac{2k_BTW_H}{\pi}\right)^{\frac{1}{4}} \left(\frac{h\upsilon_{ph}}{\pi}\right)^{\frac{1}{2}} \quad \text{for non-adiabatic hopping} \qquad (12)$$

with the condition for the existence of a small polaron having $J < \dfrac{W_H}{3}$

Using the method of successive approximation, the best fit of the eq. (11) to the corresponding experimental results (Figure 21) has been obtained for the glasses. For the (4:3:3:4) glass, for example $\hbar\omega_0 = 0.034$eV which corresponds to the phonon frequency $\upsilon_o = 8.12 \times 10^{12}$ Hz and $\theta_D = 390$K. The values of phonon frequency and Debye constants for some of the glasses are shown in Table 5. It is intersting to mention that for all these glasses phonon frequencies are about one order of magnitude smaller than those of other TMI glasses like V_2O_5–Bi_2O_3 and Fe_2O_3–Bi_2O_3, where $\upsilon_{ph} \approx 1.23 \times 10^{13}$ Hz with $\theta_D \approx$ 590K [78, 79]. It, therefore, appears that the Debye constant for these glasses are quite smaller than those of other (TMI) oxide glasses which do not become superconducting upon annealing.

It is further noted that the infrared spectra as shown in Figure 8 for the different compositions of the (4:3:3:y) type glasses are almost similar, suggesting that the optical phonon distribution does not appreciably differ in these glasses with various compositions of CuO. From the IR spectra the characteristic phonon frequency is estimated to be of the order of 1.52×10^{13} Hz corresponding to the infrared band around 500 cm^{-1} (for the (4:3:3:4) glass). This band is, however, not prominent for all the glasses. This value of phonon frequency is very close to that estimated from the electrical conductivity data viz. 8.12×10^{12} Hz. The values of υ_{ph} as given in Table 5 do not vary much with CuO concentrations indicating that the structural arrangements of all the glass compositions are similar. This also supported from the fact that the superconducting transition temperatures for these glasses do not vary appreciably from one glass composition to another [51]. The value of phonon frequency obtained from the IR spectra is, however, one order of magnitude higher than that obtained from the electrical conductivity data. This might be explained by taking the polaron correlation effect into consideration which implies that the factor $C(1-C)$ in eq. (9) should be replaced by $C(1-C)^{n+1}$. It is observed that an estimated value of phonon frequency with n = 4 is of the same order of magnitude as that obtained from the infrared spectra [51].

In eq. (11) W_p is the polaron binding energy and is related to polaron radius r_p [5, 6] as

$$W_p = \frac{e^2}{2\varepsilon_p r_p} \text{ and } W_H = \frac{e^2}{4\varepsilon_p}\left(\frac{1}{r_p} - \frac{1}{R}\right) \tag{13}$$

It turns out that a good approximation of r_p for glasses can be made by using the formula derived by Bogomolov et al [81] for the case of crystalline TiO_2 system viz.

$$r_p = \frac{1}{2}\left(\frac{\pi}{6N}\right)^{\frac{1}{3}} \tag{14}$$

The calculated value of r_p from eq. (14) are also shown in Table 3. An experimental determination of r_p is also made by taking polaron binding energy $W_P = 2W_H$ [6, 82, 83]. The values of r_P calculated by these two ways which agrees quite well [51].

The knowledge of phonon frequency υ_{ph} makes it possible to determine the small polaron coupling constant $\gamma_p = W_P/\hbar\omega_o$. For the Fe_2O_3–Bi_2O_3 and V_2O_5–Bi_2O_3 glasses it is of the order of 25. For the (4:3:3:y) type glasses γ_P varies from 8.7–14.0 depending on the CuO concentrations (Table 5). These values of coupling constants also give the polaron effective masses $m_P = m_e\exp(\gamma_P)$ (m_e being the electron mass). The polaron effective mass m_P is of the order of $10^3 - 10^6 m_e$. The numerical values of r_P, γ_P, and m_P suggest the presence of strong electron-phonon interaction and the formation of small polarons in the (4:3:3:y) or similar other glasses which become superconductors by GCR route. Thus the essential conditions for the applicability of the small polaron theory [5, 6, 77, 79] to these glasses are satisfied.

The nature of hopping in these glasses is ascertained by using the Holstein condition (eq. (12)). From the annalysis of conductivity data (Figure 21) it is possible to estimate the overlap integral J from eq. (11). Furthermore, an estimate of J can also be made from the relation

$$J \geq e^3 [N(E_F)]^{\frac{1}{2}}/\varepsilon_P^{\frac{3}{2}} \tag{15}$$

where $N(E_F)$ is the density of state at the Fermi level and

$$\frac{1}{\varepsilon_P} = \frac{1}{\varepsilon_\infty} - \frac{1}{\varepsilon_o} \tag{16}$$

where ε_∞ and ε_o are the high frequency and static dielectric constants, respectively. Polaron band width J is estimated from eq. (15) under the approximation $\varepsilon_P = \varepsilon_\infty = \mu^2$ (where μ is the refractive index of the glasses calculated from reflectance of the glasses). An estimation of $N(E_F)$ can be made by the consideration of ac conductivity of the glasses (to be discussed below) and Mott's $T^{1/4}$ analysis [5, 79] at low temperature as discussed in our

earlier paper [48]. For the (4:3:3:4) glass the estimated values of $N(E_F)$ is of the order of $1.39 \times 10^{19}\ eV^{-1}\ cm^{-3}$ Then eq. (11) gives $J \approx 0.09$ eV. The right hand side of eq. (15) is evaluated to be 0.011 eV with the values of high temperature activation energy (W_H) and

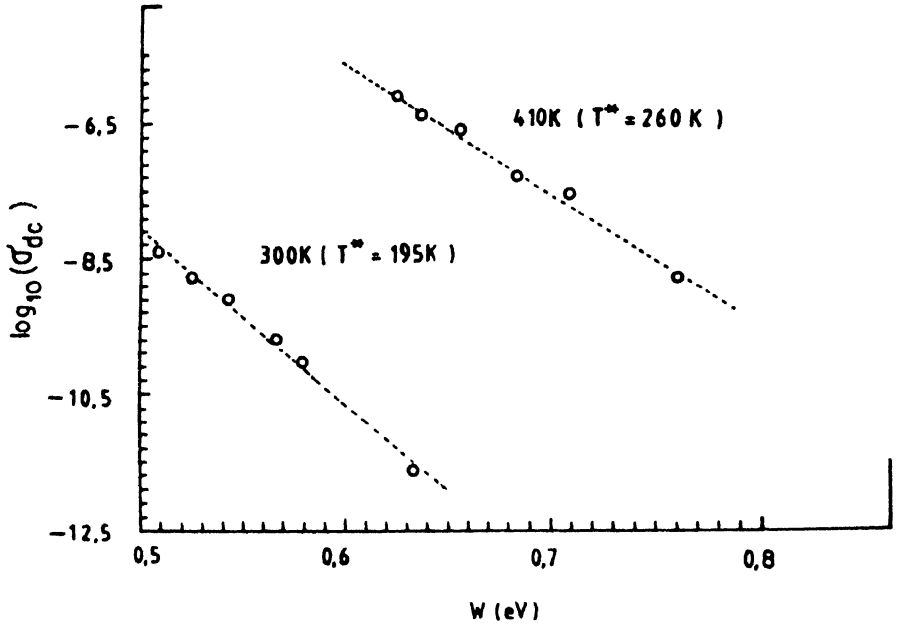

Figure 23. Variation of log σ_{dc} as a function of activation energy of the same Bi-based oxide glasses mentioned in Figure 22.

with other parameters from Table 4. Therefore, the condition for non-adiabatic hopping seems to be valid for these glasses like the Fe_2O-Bi_2O_3 glass [12] but unlike the vanadate glass [11, 78]. The observed liner dependence of log $[\sigma_0/C(1-C)]$ on R (Figure 22) also indicates the non-adiabatic hopping character for the (4:3:3:y) glasses. The same conclusion may also be drawn from the criterion of Murawski *et al* [83]. That is, the temperature T^* estimated from the slope of the log σ_{dc} versus W plot (Figure 23) should be very different from the temperature at which the conductivity data have been plotted in the figure. Here we find T^* = 260K and 195K respectively for T = 410K and 300K (at which the data were plotted in Figure 23), suggesting that the polaron hopping in these glasses is in the non-adiabatic regime. Thus the factor $J^2 \exp(-2\alpha R)$ is prevalent and cannot be neglected in the expression for the dc conductivity (eq. (8)).

Schnakenberg [84] suggested that with the lowering of temperature the multiphonon processes are replaced by a single phonon (optical phonon) process and at the lowest temperatures the polaron hops with one or more acoustic phonons making up differences between sites. The ratio of high and low temperature activation energies (W and W', respectively) is expressed as,

$$\frac{W}{W'} \quad \frac{\tanh \frac{\hbar\omega_{ph}\beta}{4}}{\frac{\hbar\omega_{ph}\beta}{4}} \tag{17}$$

where $\beta = 1/k_BT$. In Figure 24 the experimental as well as the theoretical values of W/W' given by eq. (17) are plotted against $1/T$ for the (4:3:3:4) glass. From this figure one finds that the experimental values of the activation energy decrease with increasing temperature but the quantitative fit of the experimental values with the theoretical curve is rather poor. This indicates that the increase in the magnitude of conductivity with temperature cannot be attributed to the decrease in activation energy alone.

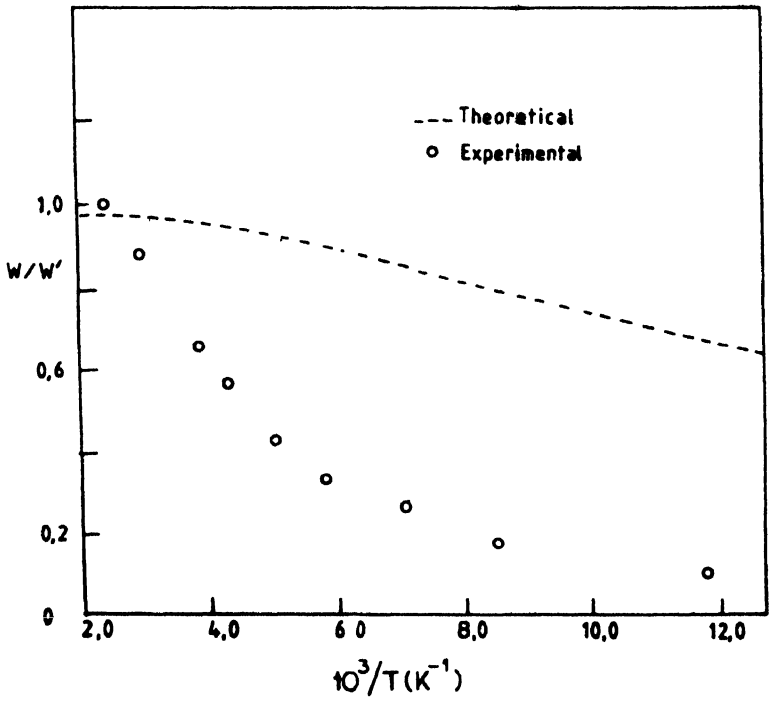

Figure 24. A plot of W/W' vs $\frac{10^3}{T}$ for (4 : 3 : 3 : 4) glasses.

At low temperature where the polaron binding energy is small and the static disorder energy of the glass plays a dominant role in the conduction process. Mott's $T^{1/4}$ analysis for the variable range hopping (VRH) can also be made. So we have plotted $T^{1/4}$ versus ln σ (Figure 25) to check the applicability of Mott's formula [5, 79] in the present (4:3:3:4) glass. According to Mott's formula the conductivity for the variable range hopping at low temperatures is given by,

$$\sigma_{dc} = A \exp(-B/T^{1/4}) \tag{18}$$

where $A = e^2N(E_F)R^2$

The slope of the $T^{-1/4}$ versus ln σ_{dc} curve gives the parameter B, where,

$$B = 2.1 \left[\frac{\alpha^3}{k_B N(E_F)} \right]^{\frac{1}{4}} \tag{19}$$

Eq. (18) suggests that the $T^{-1/4}$ versus ln (σ_{dc}) plot should be linear. The same plot for the

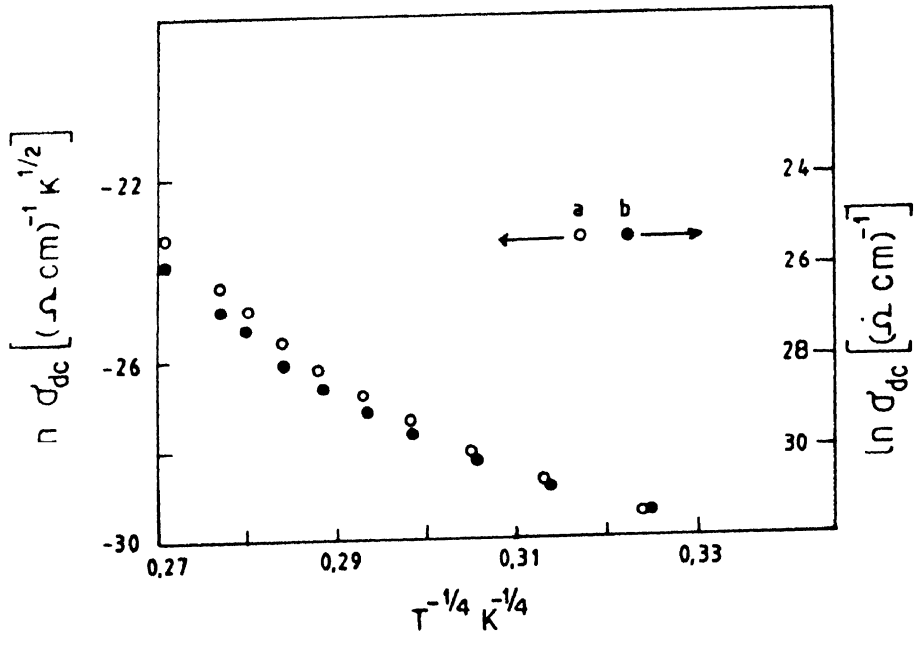

Figure 25. Plot of (a) ln σ_{dc} vs $T^{-1/4}$, and (b) ln $(\sigma_{dc} T^{1/2})$ vs $T^{-1/4}$ for (4:3:3:4) glass.

(4:3:3:4) glass (Figure 25), however, indicates the presence of two linear regions above and below $T \approx 108$K with two different slopes. From the slope of the curve below 108K and using the value of σ (obtained from fitting of experimental data with eq. (8) and shown in Table 5) the value of $N(E_F)$ is calculated to be $\approx 10^{21}$ eV^{-1} cm^{-3} which is comparatively higher than the value obtained from ac conductivity data. The disorder energy (W_D) can also be estimated from the slope of Figure 25 by,

$$B = 2.4 \left[\frac{W_D (\alpha R)^3}{k_B} \right]^{\frac{1}{4}} \tag{20}$$

The calculated value of W_D, using the value of R and α from Table 3 and Table 5, respectively, is found to be $\approx$ 1.5 eV. This value of W_D is much higher than the low temperature activation energy ($\approx$ 0.05 eV) obtained theoretically [80]. This type of high value of W_D was also reported by Dhawan *et al* [82] for the V_2O_5–TeO_2 glasses.

In an alternative way Greaves [85] suggested a variable range hopping conduction in the intermediate temperature range and derived the expression,

$$\sigma_{dc} T^{1/2} = C \exp \frac{-B}{T^{1/4}} \tag{21}$$

Here B and C are constants. B is given by the same expression as given by eq. (19). The plot of ln ($\sigma_{dc} T^{1/2}$) versus $T^{1/4}$ is shown in Figure 25 for the (4:3:3:4) glass. The straight line nature of this curve, as suggested by the Greaves relation (eq. (21)), is observed only over a small range of temperature but the general behaviour of the curve appears to deviate from linearity with the increase of temperature.

Considering the hopping within energy k_BT of the Fermi level Austin and Mott [6] obtained the expression for ac conductivity (σ_{ac}) as,

$$\sigma_{ac} = \frac{1}{3} \pi e^2 k_B [TN(E_F)]^2 \alpha^{-5} \left[\ln \frac{\upsilon_{ph}}{\omega} \right]^4 \qquad (22)$$

Substituting the values of υ_{ph} and α (from Table 5) we find $N(E_F) \approx 1.17 \times 10^{20} eV^{-1} cm^{-3}$ for 1 KHz and $N(E_F) \approx 4.17 \times 10^{19} eV^{-1} cm^{-3}$ for 10 KHz from the experimental values of $\sigma_{ac}(\omega)$ at low temperature (discussed below). These values of $N(E_F)$ for the (4:3:3:4) glass are close to the values obtained from the correlated barrier hopping (CBH) model of ac conductivity [86-87] discussed in the next section.

6.2 *AC conductivity and dielectric constant :*

The ac conductivity $\sigma_{ac}(\omega)$ and dileectric constant (ε') of the (4:3:3:4) glass have been measured between 80-420K for two different frequencies (1KHz and 10KHz). The ac conductivity $\sigma_{ac}(\omega)$ as a function of temperature is shown in Figure 26. It is observed

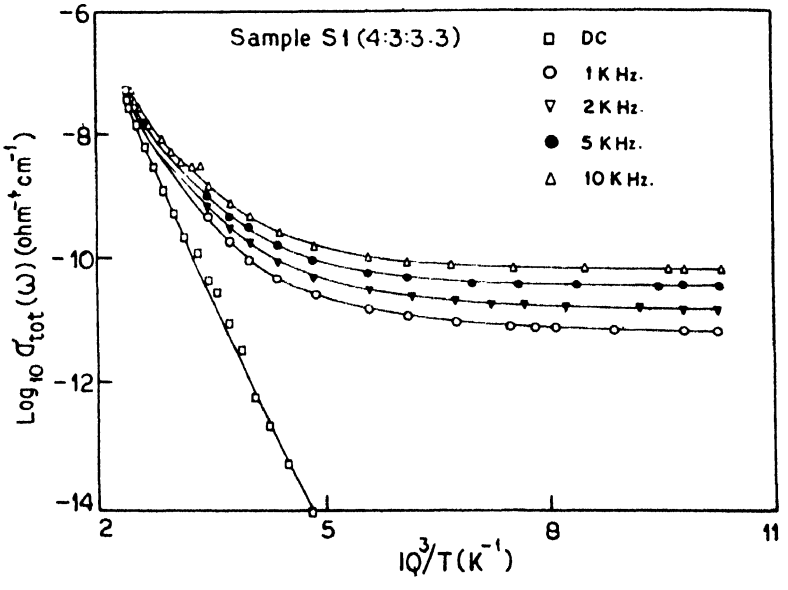

Figure 26. Variation of ac conductivities of a Bi-based glass with $\frac{1}{T}$.

from this figure that, in common with many other amorphous semiconductors, the temperature dependence of $\sigma_{ac}(\omega)$ is much less than σ_{dc} at low temperatures and is not

activated in behaviour. However, the temperature and its frequency dependences become strong with the increase of temperature. Ultimately, the measured conductivities at all frequencies coincide with σ_{dc} at higher temperatures.

The ac conductivity as shown in Figure 26 was calculated by subtracting the measured dc conductivity from the measured total frequency dependent conductivity $\sigma_t(\omega)$ such that

$$\sigma_{ac}(\omega) = \sigma_t(\omega) - \sigma_{dc} \tag{23}$$

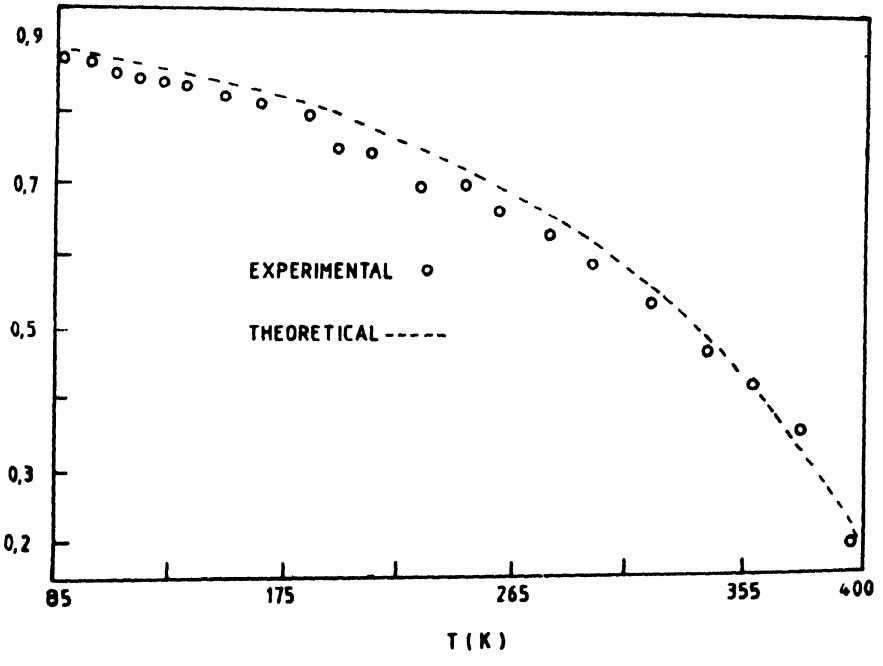

Figure 27. Temperature variation of σ of the glasses (4 : 3 : 3 : 4) at 1 KHz. (0) experimental points, and (———) theoretical curves obeying eq. (36).

When ac and dc conductivities are due to the same process and σ_{dc} is simply $\sigma_{ac}(\omega)$ (in the limit $\omega \to 0$), the separation given in eq. (23) is no longer useful.

Like many amorphous semiconductors and insulators, the ac conductivity of the (4:3:3:4) glass was found to follow the equation

$$\sigma_{ac}(\omega) = A\,\omega^{s} \tag{24}$$

where A is a constant dependent on temperature and s is the frequency exponent, generaly less than unity. All that is required to give this behavior is that the loss mechanism should have a very wide range of possible relaxation times.

The estimated frequency exponent s is shown in Figure 27 as a function of temperature. The variation of the exponent s at room temperature with frequency is shown in Figure 28. It is interesting to mention that such a sharp frequency dependence of s has not been observed for the vanadate or similar other oxide glasses [11, 12, 76, 88].

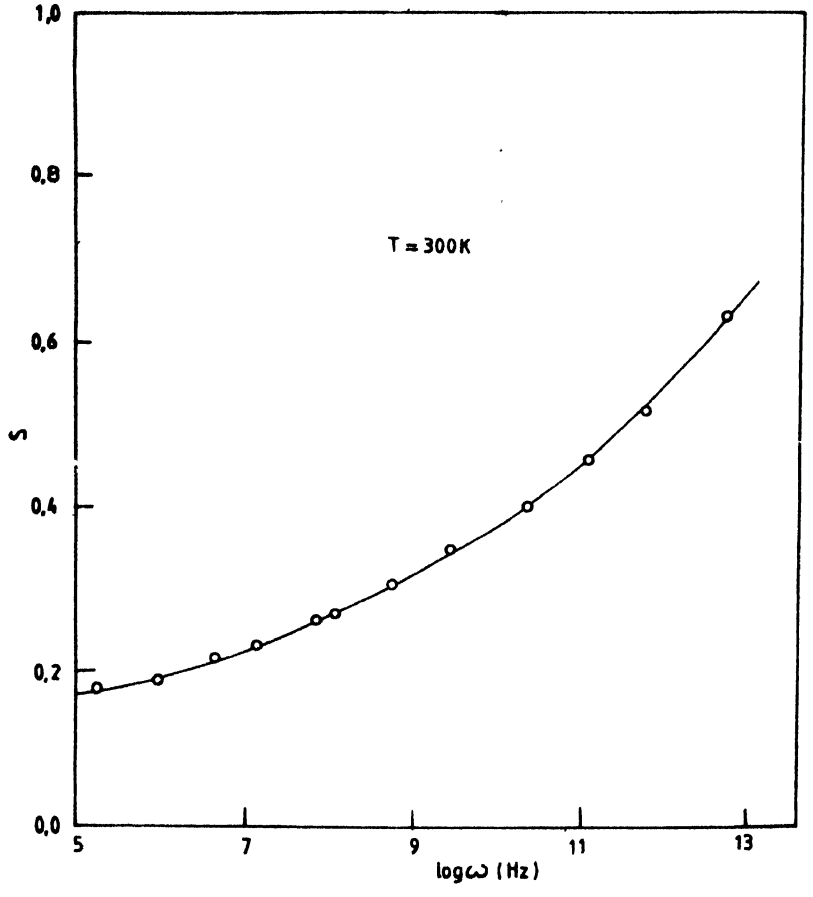

Figure 28. Variation of s with frequency at room temperature (300K).

Many different theoretical explanations [86, 87] for the ac conduction in amorphous semiconductors have been proposed to account for the frequency and temperature dependence of σ_{ac} and s. It is commonly believed that the pair apprioximation holds, namely the dielectric loss occurs because the carrier motion is considered to be localized within pair of sites. In essence, two distinct processes have been proposed for the relaxation mechanism, namely quantum mechanical tunnelling through the barrier separating two equilibrium positions and classical hopping of a carrier over the barrier or some combination or variant of the two, and it is variously assumed that the electrons (or polarons) or atoms are the carriers responsible for the conduction. In what follows, the ac conductivity data for the

(4:3:3:4) glassy semiconductor are analysed in the light of the existing theoretical models.

(A) Quantum mechanical tunnelling (QMT) model :

Several authors [6, 87, 89, 90] calculated with the pair approximation, the ac conductivity data for single electron motion undergoing QMT and obtained the expression for the ac conductivity as

$$\sigma_{ac}(\omega) = Ce^2 k_B T \alpha^{-1} [N(E_F)]^2 \omega R_\omega^4 \tag{25}$$

where C is a numerical constant, and R_ω is the hopping distance at frequency ω, given by

$$R_\omega = (2\alpha)^{-1} \ln \frac{1}{\omega\tau_o} \tag{26}$$

where τ_o is a characteristic relaxation time. The frequency exponent s in this model is obtained from

$$s = 1 - \frac{4}{\ln(\omega\tau_o)} \tag{27}$$

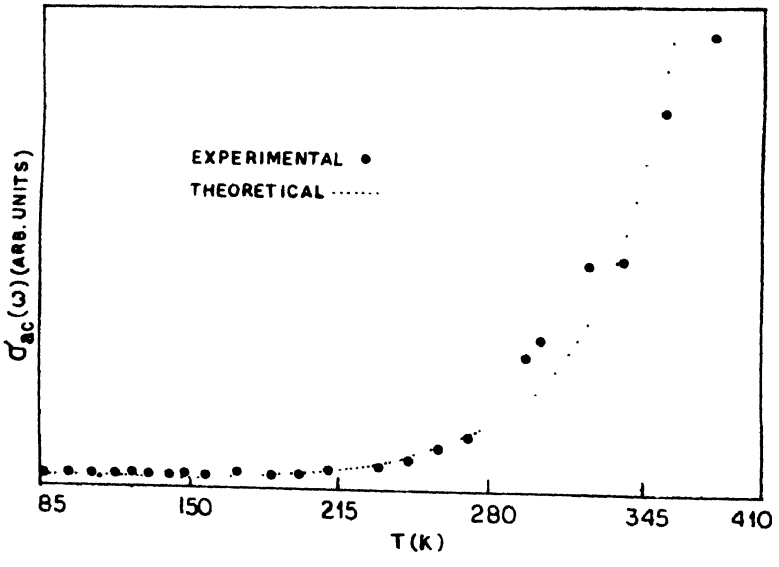

Figure 29. Thermal variation of $\sigma_{ac}(\omega)$ at 1KHz. ; (●) experimental points and (----------) theoretical curve obeying CBH model.

Therefore, for the QMT model, $\sigma_{ac}(\omega)$ is linearly dependent on temperature T [eq. (25)], but the exponent s is temperature independent and frequency dependent [eq. (27)]. For typical values of the parameters $\tau_o = 10^{-13}$ sec and $\omega/2\pi = 10^4$ Hz, a value of $s = 0.81$ is obtained from eq. (27). However, it is clearly observed for the (4:3:3:4) glass that the exponent s

decreases with increase of temperature (Figure 27) and increases with increase of frequency at a fixed temperature (Figure 28). Furthermore, QMT model predicts a linear temperature dependence of $\sigma_{ac}(\omega)$. But our experimental results, as shown in Figure 29 indicate a much sharper increase of $\sigma_{ac}(\omega)$ with the rise of temperature particularly in the high temperature regime. A temperature dependent frequency exponent can be obtained within the framework of the QMT model by assuming that the carriers form non-overlapping small polarons. In our case, however, the frequency exponent deceases with increase in temperature (Figure 28). The simple QMT model also predicts that s should decrease with increase of frequency [eq. (27)]. But in (4:3:3:4) glassy semiconductor s increases sharply with frequency in the range of our investigation viz. (10^2–10^5 Hz). Thus for the above reasons the QMT model clearly fails to explain the experimental ac conductivity data of the (4:3:3:4) glass.

(B) Overlapping polaron tunnelling (OPT) model :

In this case, as suggested by Long [87] the large polaron wells of the two sites overlap and thereby reduces the polaron hopping energy. In this case one has

$$W_H = W_{HO}\left(1 - \frac{r_p}{R}\right) \tag{28}$$

where W_{HO} is defined as

$$W = \frac{e^2}{4\varepsilon_p r_p} \tag{29}$$

Assuming R as a random variable, $\sigma_{ac}(\omega)$ in this model [87] comes out to be of the form

$$\sigma_{ac}(\omega) = \frac{\pi^4}{12} e^2 (k_B T)^2 [N(E_F)]^2 \bar{x} \tag{30}$$

where $$\bar{x} = \frac{\omega R_\omega^2}{\left(2\alpha k_B T + W_{HO} r_p / R_\omega^2\right)}$$

The hopping length R_ω is determined from the quadratic equation

$$(R_\omega) + [\beta W_{HO} + \ln(\omega\tau_0)] R_\omega' - \beta W_{HO} r_p' = 0 \tag{31}$$

Here $R_\omega' = 2\alpha R_\omega$, $r_p' = 2\alpha r_p$, and $\beta = \frac{1}{k_B T}$

The exponent s in the OPT model can be evaluated from

$$1 - s = \frac{8\alpha R_\omega + \frac{6\beta W_{HO} r_p}{R_\omega}}{\left(2\alpha R_\omega + \frac{\beta W_{HO} r_p}{R_\omega}\right)^2} \tag{32}$$

Thus the OPT model predicts that s should be both temperature and frequency dependent [cf

eq. (32)] and that the frequency exponent s decreases from unity with the increase of temperature. For large values r_p''s the values of s continue to decrease with increasing temperature, eventually tending to the value of s predicted by the simple QMT model, where for small values of r_p''s the exponent s exhibits a minimum at a certain temperature

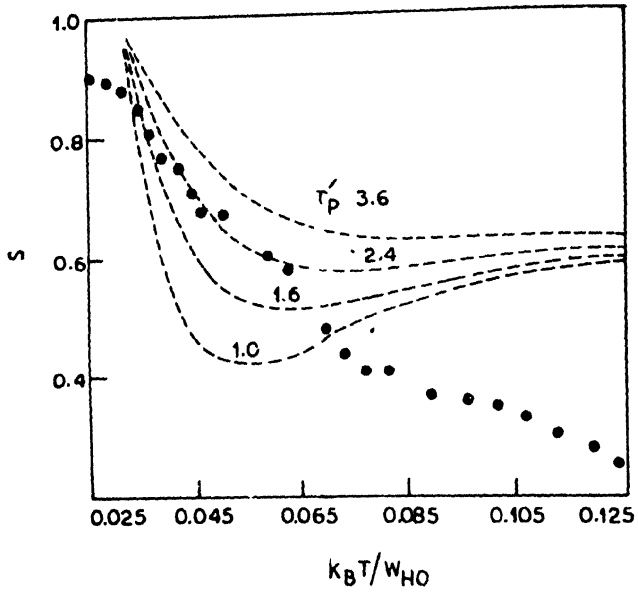

Figure 30. Plot of $\frac{k_BT}{W_{HO}}$ vs s; (●) experimental points and (----------) theoretical curve.

and subsequently increases in a similar fashion as in the case of small polaron QMT. Thus, it appears that the OPT model should better fit the experimental ac conductivity data of the (4:3:3:4) glass, since the experimental values of s decreases with the increase of temperature (Figure 27). To verify this, the frequency exponent s is plotted in Figure 30 as a function of k_BT/W_{HO} similar to our earlier paper on the semiconducting oxide glasses [11, 12]. The value of W_{HO} was calculated from eq. (29) using the values of r_P and ε_P from dc conductivity data (shown in Table 3). The theoretical curves given by eq. (32) are also drawn in Figure 30 for various values of r_p'. The best fit to the experimental data (in the low temperature region, for $k_BT/W_{HO} < 0.6$) has been observed for the value of $r_p' = 2.4$ as shown in Figure 30. The decay constant α can be estimated from the relation $r_p' = 2\alpha r_P$ using this value of r_p'. The estimated value of α agrees fairly well with the value obtained from the dc conductivity data [48]. However, the values of r_P, being smaller than R, appears to be inconsistent with the basic premise of the OPT model (for the large polaron case). At higher temperatures, the experimental data for S neither lie between the theoretical curves (Figure 30), nor they show minimum according to the requirement of the OPT model. This is also true for the V_2O_5–Bi_2O_3 [11] and Fe_2O_3–Bi_2O_3 [12] glasses.

The OPT model also predicts [cf. eq. (30)] an appreciably stronger temperature dependence of $\sigma_{ac}(\omega)$ in the temperature regime where the frequency exponent s is a decreasing function of temperature. The functional form of the temperature dependence of $\sigma_{ac}(\omega)$ shown by eq. (20) is a complicated one and cannot be expressed simply as T^{υ} (with υ constant over a wide range of temperature). Nevertheless, at low temperatures ($k_BT/W_{HO} <$ 0.04 – 0.05) the hopping length R has an approximately constant temperature dependence, $R \sim T^{1.25}$ (for $r_P \approx 2.5$) and insertion of this value in eq. (30) yields $\sigma_{ac}(\omega) \sim T^6$ for the uncorrelated case. This is obviously at variance with the much weaker temperature dependence exhibited by the low temperature data of the present work (Figure 29) and even if the correlated form [86] of OPT model is invoked, the said dependence is predicted to decrease only to $\sigma_{ac}(\omega) \sim T^4$. It therefore, appears that the temperature dependence of the ac conductivity is not really met within the framework of the OPT model developed by Long [87].

(C) Correlated barrier hopping (CBH) model :

Another model for ac conductivity which correlates the relaxation variable W with the intersite separation R was proposed by Pike [89] for single electron hopping and extended by Elliott [86] for the two electrons hopping simultaneously. For the neighbouring sites at a separation R, the Coulomb wells overlap, resulting in a lowering of the effective barrier height from W_M to a value W, which for the case of two electrons hopping is given by [86, 87]

$$W = W_M - \frac{2e^2}{\pi\varepsilon\varepsilon_o R} \tag{33}$$

where ε and ε_o are, respectively, the dielectric constant of the material and the permittivity of the free space. The ac conductivity in this CBH model, in the narrow band limit, is given by [86, 87]

$$\sigma_{ac}(\omega) = \frac{1}{24}\pi^3 N\varepsilon_o\varepsilon R^6_{\omega} \tag{34}$$

The hopping distance R_ω is given by

$$R_\omega = \frac{2e^2}{\pi\varepsilon\varepsilon_o}\left[W_M - k_BT \ln\left(\frac{1}{\omega\tau_o}\right)\right] \tag{35}$$

The frequency exponent s with the CBH model is given by

$$1 - s = \frac{6k_BT}{W_M - k_BT \ln\left(\frac{1}{\omega\tau_o}\right)} \tag{36}$$

Therefore, according to the CBH model a temperature dependent frequency exponent s is predicted, with s increasing towards unity as $T \to 0$, which is in marked contrast with the QMT or simple hopping over barrier model [87], and therefore, it might be a possible

contending model for the explanation of the ac conductivity of the (4:3:3:4) glass in its semiconducting phase.

A critical test of the CBH model comes from the temperature dependence of the ac conductivity and its frequency exponent. Our experimental results, as shown in Figures 27 and 29 show exactly similar nature as suggested by the CBH model. In Figure 27 the experimental values of s are shown as a function of temperature along with the theoretical curve obeying eq. (36) with $\omega/2\pi = 1000$ Hz and $W_M = 0.88$ eV. Here W_M is taken as twice the high temperature activation energy obtained from our dc conductivity results as shown in Table 4. The best fit with the experimental curve is obtained with $\tau_o = 10^{-12}$ sec which seems to be quite reasonable and nearly equal to the values obtained for other semiconducting oxide glasses [9, 12, 87]. The little discrepancy existing between the theoretical and the experimental values as indicated by Figure 27 might be due to some inaccuracy in the determination of the barrier height (W_M). At this point it would be worthwile to mention that the correlation between the barrier height and hopping distance might cause appreciable deviation of $\sigma_{ac}(\omega)$ as well as of s from the corresponding theoretical values. Using the same value of W_M (= 0.88 eV) and τ_o (= 10^{-12} sec) we have calculated the value of R_ω from eq. (35) which was found to be $\approx 7.7 \times 10^{-8}$ cm. Putting this value of R_ω and ε from our experimental dielectric constant data in eq. (34), N was calculated to be $\approx 1.39 \times 10^{19}$ eV^{-1} cm^{-3}. The estimated value of N [48] seems to be rather low which may be due to the fact, as suggested by Linsley *et al* [19], that some of the sites may remain inactive due to glass structure resulting in a lower number of sites actually participating in the conduction process.

The temperature dependence of $\sigma_{ac}(\omega)$ in the CBH model is given by

$$\sigma_{ac}(\omega) \alpha T^{\upsilon} \tag{37}$$

where $$\upsilon = (1 - s) \ln \frac{1}{\omega\tau_o} \tag{37a}$$

In Figure 29 we have plotted the experimental temperature variation of $\sigma_{ac}(\omega)$ along with the theoretical temperature dependence obeying eq. (37). A reasonably good fitting of the experimental values with the theoretical curve indicates the applicability of the CBH model in explaining the experimental ac conductivity data of the (4:3:3:4) glass.

6.3. *Dielectric constant :*

The dielectric constant (ε') and the loss tangent tan δ, were also measured simultaneously along with the ac conductivity measurement using capacitance bridge technique as discussed earlier.

The temperature variation of ε' and tan δ for two fixed frequencies 1kHz and 10kHz are shown in Figure 30. Both ε' and tan δ are found to increase with the increase of temperature. The curve corresponding to 10kHz (Figure 31) shows a peak at about 366K in the ε' versus T curve which is a common feature indicating Debye type dielectric relaxation

process [92, 93] characterized by a relaxation frequency f_o (where $f_o = 1/2\pi\tau_o$, τ_o being the dielectric relaxation time). The loss peak occurs at a temperature at which the measuring

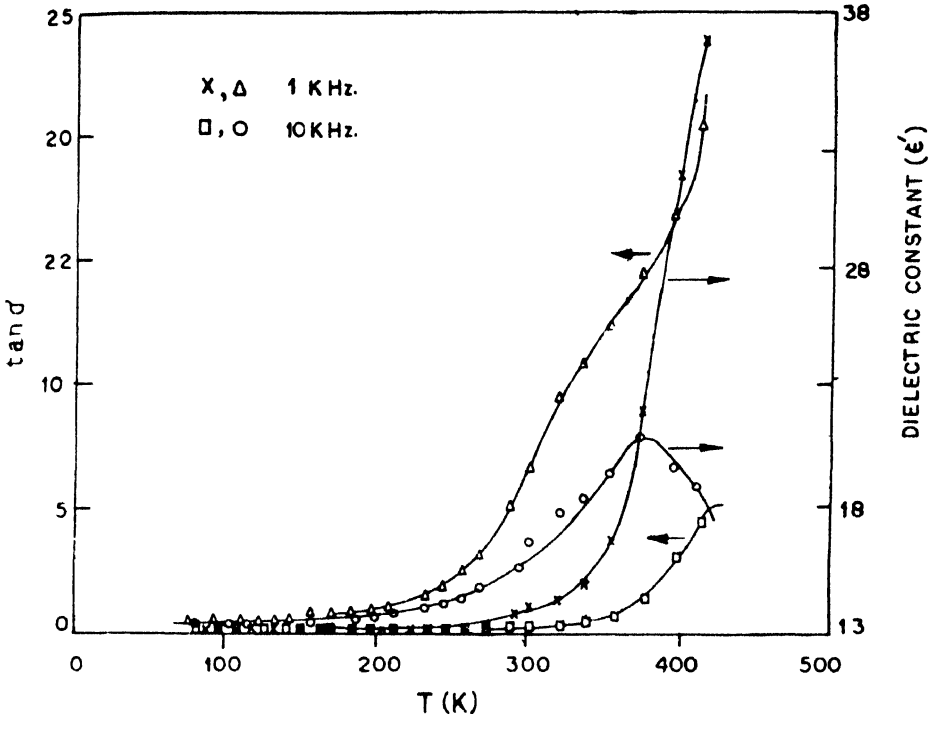

Figure 31. Temperature variation of dielectric constants and tan δ for the Bi-based (4 : 3 : 3 : 4) glasses at two different frequencies.

frequency equals the relaxation frequency. For this (4:3:3:4) glass the loss curve corresponding to 1kHz shows no such peak within the range of our investigation. In Figure 32 we have plotted ε′ versus ln (ω) as well as tan δ versus ln (ω) at room temperature (300K). Both ε′ and tan δ are found to decrease with increase of frequency which are consistent with the behaviour of ac conductivity discussed above.

6.4. *Imaginary part of ac conductivity :*

Real (denoted by σ_1 (ω)) and the imaginary part (denoted by σ_2 (ω)) of the ac conductivity are related via Kramers-Kronig relation. The values of σ_1 (ω) and σ_2 (ω) are also related to the dielectric constant. The total measured capacitance C_{tot} (ω), like conductance, can also be expressed into two parts, arising from different processes, viz.

$$C_{tot}(\omega) = C(\omega) + C_\infty \tag{38}$$

where the dispersive term $C(\omega)$ is determined by the loss measurements and the non-dispersive term C_∞ is determined by the high frequency atomic and dipolar vibrational

transitions. Serveral methods [87] for determining $C(\omega)$ from the capacitance data have been proposed. In the present work, $C(\omega)$ was estimated from the numerical differentiation of the capacitance whereupon the constant term involving C_∞ drops out. The ratio of the imaginary to the real part of the conductivity is then calculated from the relation,

$$\lambda = \frac{\sigma_2(\omega)}{\sigma_1(\omega)} = \frac{\omega C(\omega)}{G(\omega)} \tag{39}$$

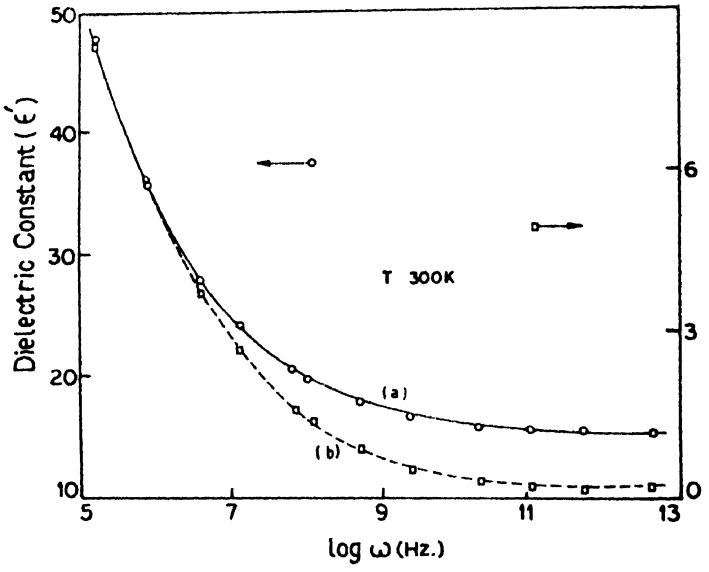

Figure 32. Frequency variation of (a) ε' (0) and (b) tan δ ($\square$) of the (4 : 3 : 3 : 4) glass at 300K.

where $G(\omega)$ is the conductance at frequency ω. It has been shown [87] that λ have characteristically different forms for the various mechanisms of dielectric relaxation. Thus from the QMT model one finds

$$\lambda = -\frac{2}{\pi} \ln(\omega\tau_o) \tag{40}$$

and the CBH model, on the otherhand, gives to a first approximation for small k_BT/W_M,

$$\lambda = -\frac{2}{5\pi} \ln(\omega\tau_o) \left[1 + \frac{3k_BT}{W_M} \ln(\omega\tau_o)\right] \tag{41}$$

It might be noted that the CBH model predicts a temperature dependence of λ, whereas the QMT model does not. For the OPT model λ behaves like that for the QMT model at high temperatures and at low temperatures the behaviour is similar to that exhibited by the CBH model.

Calculation of the ratio λ using our experimental data indicates that λ is temperature dependent which implies inapplicability of the QMT model for the (4:3:3:4) glass.

However, for the CBH model (eq. (41)) the fit between theory and experiment is found to be reasonably good which supports the applicability of the CBH model for the ac conductivity data of the (4:3:3:4) glassy semiconductor. However, it should be noted that eq. (41) for the CBH model is also an approximate one ; higher order terms become important at higher temperatures.

7. Preparation of (HITSO) wires, tapes, and films from glass

It has already been mentioned that there is immense possibilities [20, 72, 94-97] of making (HITSO) wires, tapes or films from the glass phases. Several reports for the preparations of thick films [35, 47, 23, 65, 67], thin films [31], wires or fibers [94, 96, 97] etc. have already been made in the current literature. Thin films could be made by pouring the melt on suitable substrates and then annealing the films in oxygen atmosphere at a suitable temperature depending on the thickness of the films. Reports on the preparation of rods by pouring the glass melt inside the ceramic or metallic tubes have been made [51, 95]. This rod could be converted into the corresponding superconducting phase by annealing it above the glass transition temperature but below its melting point. It is found easier to draw wires or fine fibers from this glass rod by quickly pulling a small melted part (better with laser beam) of the rod.

The melted Y–Ba–Cu–O or the Bi–Sr–Ca–Cu–O etc. oxides become just like water and are found very inconvenient for drawing wires or tapes directly from the melt unlike the vanadium or iron oxide based (TMI) glasses. Presence of little amount of glass formers like B_2O_3, MgO, Bi_2O_3 (in case of Y–Ba–Cu–O system) etc. are found to improve the viscous character. The addition of glass former also found to improve the stability of the oxygen content in the Y–Ba–Cu–O superconductor. Unfortunately, the addition of such a glass former supersses the superconducting transition temperature by about 10-20K (for an addition of ~ 5 mol % of B_2O_3 or MgO in the glass). Komatsu *et al* [99] studied the effect of MgO addition on the superconducting behaviour of Y–Ba–Cu–O. It was found that both T_c (93K)and T_{co} (90K) decreased from 93K to 75K and 90K to 70K, respectively for an addition of 5 mol % of MgO. However, for the $(Ba_{1-x}Mg_x)_2YCu_3O$ system the values of T_c do not change appreciably if x is kept within 0.05. These results are useful for understanding the superconducting properties of $YBa_2Cu_3O_x$ thin films prepared on the MgO substrate [30, 99,100]. Recently it has also been reported by Meng *et al* [98] that high J_c (~ 3×10^4 A/cm^2 or more) valued bulk (1:2:3) superconductor could be prepared by the melt process. It is found, however, that [4:3:3:4] and other glasses doped with alkali atoms show higher T_c [105–107] by 5–9K with better microstructures of the HITSO phases in their respective glass ceramics.

Though the critical current density of the superconducting thick films or wires prepared from the glass phases are low (50-200 A/cm^2), recently Murakami *et al* [20] developed a new technique for making oriented thin films from the melt glass with the promise of high J_c in the Y–Ba–Cu–O system They developed films of J_c value exceeding

10^4 A/cm^2 at 77K and at a magnetic field of 1T indicating the high potential of oxide superconductors as a candidate for technological applications. However, one should mention that all the techniques developed so far for the preparations of HITSO tapes, films or wire are in the rudimentary stage with a promise of high technological applications.

8. Summary and conclusion

In the present review we have discussed in details the preparation and characterization techniques of Y–Ba–Cu–O and Bi–Sr–Ca–Cu–O based trasition metal oxide glasses which become superconductors unlike the vanadate or other transition metal oxide glasses upon annealing at a temperature just below their melting points (T_m). The high temperature superconducting materials obtained from this glass to ceramic route are highly dense and less porous than those obtained from the usual ceramic technique. There is also great possibility of making wires, ribbons or fibres from these glasses and then converting them to the corresponding superconducting phases by annealing. However, adequate technology for the preparation of high quality films or wires using the glass to ceramic route has yet to be developed.

High density, relatively low glass transition temperature (T_g), and very low conductivity of these oxide glasses distinguishes them from the vanadate or orther transition metal oxide glasses. However, the general behaviour of all the oxide glasses as a function of temperature and/or frequency are found to be almost similar. Finally we would like to mention that we have reported mostly the properties of the bulk materials in their glassy and ceramic phases. For a thorough understanding of the mechanism which makes these glasses superconducting upon annealing one should also study intensively the microstructural properties, grain boundary effects, etc. for different concentrations of these glasses. Studies of concentration dependences of the superconducting transition temperatures, structure of the glasses etc. are yet to be carried out for different systems. However, it might be concluded that there is immense scope for such studies and further developement of the glass to ceramic route for making (HITSO) tapes or films for their application in tomorrow's technology.

Acknowledgment

The authors are grateful to Professors S Ray, R N Bhattacharya, and Professor U S Ghosh, Head of the Department of Solid State Physics, for their interest and encouragement in this work. Sincere help from other colleagues and students is also gratefully acknowledged. The authors are also grateful to Professor S P Sengupta for allowing them to do XRD studies in his laboratory. The authors are grateful to DST and QSIR for financial supports to Complete the work.

References

1. H Hirashima, Y Watanabe and T Yoshida, *J Non-Cryst. Solids* **95 & 96** (1987) 825
2. A Ghosh, Ph.D. Thesis, (1986), *Jadavpur University*, Calcutta

3. Y Sakuri and J Yamaki, *J Electrochem Soc* **132** (1985) 512
4. S Nakamura and N Ichinose, *J Non-Cryst. Solids* **95 & 96** (1987) 849
5. N F Mott and E A Davis, 1979 *"Electronic Processes in Non-Crystalline Materials"*, 2nd ed (Oxford : Clarendon)
6. I G Austin and N F Mott, *Adv. Phys.* **18** (1969) 41
7. M Sayar and A Mansingh, *Phys. Rev.* **B6** (1972) 4629
8. J D Mackenzie (1964) *"Modern Aspects of Vitreous State"*, Vol. 3 (London : Butterworth) p. 126.
9. C Chung, J D Mackenzie and L Mruawski, *Rev de chim. Miner* **16** (1979) 308
10. K W Hansen and M Splann, *J Electrochem. Soc.* **113** (1966) 9
11. A Ghosh and B K Chaudhuri, *J Mater Sci.* **22** (1987) 2367
12. B K Chaudhuri, K Chaudhuri and K K Som, *J Phys. Chem. Solids* **50** (1989) 1137, 1155
13. C F Drake, I F Scanlan and A Engel, *Phys. Stat. Solidi* **32** (1969) 193
14. C F Drake and I F Scanlan, *J Non-Cryst Solids* **4** (1970) 234
15. I G Austin and M Sayer, *J Phys* C7 (1972) 905
16. A Duran, J R Jurado and J M F Navarro, *J Non-Cryst Solids* **79** (1986) 333, 352
17. T Tsuchiya and T Mony, *Cent glass ceram Res Inst. Bull* **22** (1975) 2, 55
18. T Komatsu, K Imai K Matusita, M Tanaka, Y Iwai, A Kawakami, Y Kaneko and T Yamashita, *Jpn J Appl. Phys. Lett.* **26** (1987) L1272, L1148
19. H S Koo, T Y Tseng, R S Liu and Y T Wu, *Jpn. J Appl Phys. Lett.* **28** (1989) L41
20. M Murakami, M Morita, K Doi and K Miyamoto, *Jpn J Appl Phys. Lett.* **28** (1989) L1189
21. J S Luo, D Michel and J P Chevalier, *Appl. Phys Lett* **55** (1989) 1448
22. H Zheng and J D Mackenzie, *Phys. Rev.* **B38** (1989) 7166
23. B K Chaudhuri, K K Som and S P Sengupta, *J Mater. Sci Lett* **8** (1989) 520
24. T Komatsu, T Ohki, C Hirose and K Matusita, *J Non-Cryst Solids* **113** (1989) 274
25. H Nasu, Y Ibara, S Makida, T Imura and Y Osaka, *J. Non-Cryst Solids* **105** (1988) 185
26. D Shi, M Tang, K Vandervoort and H Claus, *Phys. Rev* **B39** (1989) 9091
27. T Minami, Y Akamatsu, M Tatsumisago, N Tohge and Y Kowada, *Jpn. J Appl Phys Lett.* **27** (1988) L777
28. M Tatsumisago and C A Angell, *Appl Phys. Letts.* **55** (1989) 600, 2268
29. H Konishi, T Takamura, H Kaga and K Katsuse, *Jpn. J Appl. Phys Lett.* **28** (1989) L241
30. H M Jang, K W Moon and S Baik, *Jpn J Appl. Phys. Lett* **28** (1989) L1223
31. M Yoshimura, T Sung, Z Nakagawa and T Nakamura. *Jpn. J Appl. Phys Lett* **27** (1988) L1877
32. Y Ibara, H Nasu, T Imura and Y Osaka, *Jpn. J Appl. Phys. Lett* **28** (1989) L37
33. T Komatsu, R Sato, K Imai, K Matusita and T Yamashita, *IEEE Trans. Mag.* **25** (1989) 2150
34. T Komatsu, R Sato and K Matusita, *Appl. Phys. Lett.* **54** (1989) 1169
35. T Komatsu, R Sato, K Imai, K Matusita and T Yamashita, *Jpn J Appl. Phys Lett* **27** (1088) L550, L533
36. L I Maissel and R G Glang, (1970) *"Handbook of Thin Film Techonology"* (New York : McGraw Hill)
37. G N Jackson, *Thin Solid Films* **5** (1970) 209
38. P W Mcmillan, (1964) *"Glass Ceramics"* (New York : Academic)
39. P Duwez and R H Willens, *Trans. Soc.* AIME **227** (1963) 362
40. H S Chung and C E Miller, *Rev. Sci. Instsum.* **41** (1970) 1237
41. A E Owen, (1973) *"Electronic and Structural Properties of Amorphous Semiconductor"* eds. P G Lecomber and J Mort (New York : Academic) p 161
42. P T Sarjent and R Roy, *Mater Res. Bull.* **3** (1968) 265
43. D Turnbull and M H Cohen, *J. Chem. Phys* **52** (1970) 3038, *ibid.* **34** (1961) 120
44. G Adams and J H Gibbs, *J. Chem. Phys.* **43** (1965) 139
45. C A Angell and K L Rao, *J. Chem. Phys.* **52** (1972) 470
46. V Skumryev, R Puzniak, R Puzniak, N Karpe, H Zheng-He, M Pont, H Medelius, D X Chen and K V Rao, *Physica* **C152** (1988) 315
47. S Shimomura, A Takahashi, M Ohta, A Watanabe, M Seido and F Hosono, *Jpn. J. Appl. Phys. Lett.* **27** (1988) L1890

48. K K Som and B K Chaudhuri, *Phys. Rev.* **B41** (1990) 1581
49. A Inoue, H Kimura, K Matsuzaki, A Tsai and T Matsumoto, *Jpn. J. Appl. Phys. Lett.* **27** (1988) L941
50. K B R Varma, K J Rao and C N R Rao, *Appl. Phys. Lett.* **54** (1989) 69
51. B K Chaudhuri and K K Som, *Proc. Int. Conf. High Temp. Superconductivity, Bangalore* (India), *Jan. 10-14*, 1990 (to be published in Mater Sci. Bull.)
52. H Zheng, R Xu and J D Mackenzie, *J Mater Res.* **4** (1989) 911
53. T Kanai, T Kumagai, A Soeta, T Suzuki, K Aihara, T Kamo and S Matsuda, *Jpn. J. Appl. Phys. Lett.* **27** (1988) L1435
54. D G Hinks, L Soderholm, D W Capone, B Dabrowski, A W Mitchell and D Shi, *Appl. Phys. Lett.* **53** (1988) 423
55. K B R Varma, G N Subbanna, T V Ramakrishnan and C N R Rao, *Appl. Phys. Lett.* **55** (1989) 75
56. K Matsusita and S Sakka, *J. Non-Cryst Solids* **38 & 39** (1980) 741
57. B K Chaudhuri and K K Som (unpublished)
58. Z Xu, P D Han, L Chang, A Asthana and D A Payne, *J. Mater. Res.* **5** (1990) 39
59. D Shi, M Tang, M S Boly, M Hash, K Vandervoot, H Claus and Y N Lwin, *Phys. Rev.* **B40** (1989) 2247
60. H Takei, M Koike, H Takeya, K Suzuki and M Ichihara, *Jpn. J. Appl. Phys. Lett.* **27** (1988) L1237
61. T Ishida and T Sakuma *Jpn. J Appl. Phys. Lett.* **27** (1988) L1237
62. H Rawson, (1967) *"Organic Glass Forming System"* (London : Academic)
63. S Lindqvist, E Tosatti, M Tosi and Yu Lu, (1987) (eds) *Proc. Adriatico Reserach Conference on High Temperature Superconductivity* Vol. 1
64. P N Bansal and D E Farrell, *J. Appl. Phys. Lett* **55** (1989) 1572
65. Y Akamatsu, M Tatsumisago, N Tohge, S Tsuboi and T Minami, *Jpn. J. Appl. Phys. Lett.* **27** (1988) L1696
66. B K Chaudhuri and K K Som (1990) *Proc. Int. Conf. on Cryogenics*, Calcutta, December 6-10, 1988 eds A Bose and P Sengupta (New Delhi : Macmillan India) p 151
67. K J Kwon, Z S Lim, T Y Kim, J K Son and S I Lee, *Physica* **C159** (1989) 659
68. T Ishida, *Jpn. J. Appl. Phys. Lett.* 28 (1989) L197
69. B M Moon, B Lalevic, B H Kear, L E Mccandlish, A Safari and M Meskoobn, *Appl. Phys. Lett.* **55** (1989) 1466
70. B K Chaudhuri (unpublished)
71. W Gao, S C Li, D A Rudman, G J Yurek and J B V Sande, *Appl. Phys. Lett.* **55** (1989) 2227
72. R C Baker, W H Hung and H Steinfink, *Appl. Phys. Lett.* **54** (1989) 371
73. A R Yavari and P Lejay, *J. Crystal Growth* **91** (1988) 290
74. O L Krivanek, P H Gaskell and A Howie, *Nature* **262** (1976) 454
75. B K Chudhuri, *Proc. National Conf. Cryogenics, March*, 1990, *Banaras Hindu University, India*
76. A Ghosh and B K Chaudhuri, *J. Non-Cryst. Solids* **83** (1986) 151
77. T Holstein, *Ann. Phys.* **8** (1959) 343
78. A Ghosh and B K Chaudhuri, *J Non-Cryst. Solids* **103** (1988) 83
79. N F Mott, *J. Non-Cryst. Solids* **1** (1968) 1
80. A Miller and E Abrahams, *Phys. Rev.* **120** (1960) 745
81. V N Bogomolov, E N Ksudinov and A Yu Firsov, *Soviet Phys. Solid St.* **9** (1967) 3175
82. V K Dhawan and A Mansingh, *J. Non-Cryst. Solids* **51** (1982) 87
83. L Murawski, C H Chung and J D Mackenzie, *J Non-Cryst. Solids* **32** (1979) 91
84. J Schnakenberg, *Phys. Stat. Solids* **28** (1968) 623
85. G N Greaves, *J. Non-Cryst. Solids* **11** (1973) 427
86. S R Elliott, *Phil. Mag.* **36** (1977) 1291; *Adv. Phys.* **36** (1987) 135
87. A R Long, *Adv. Phys.* **31** (1982) 553
88. C H Chung and J D Mackenzie, *J. Non-Cryst. Solids* **42** (1980) 357
89. G E Pike, *Phys. Rev.* **B6** (1972) 1572
90. A L Efros, *Phil. Mag.* **B43** (1981) 829
91. G S Linley, A E Owen and F M Hayattaite, *J. Non-Cryst. Solids* **4** (1970) 208

92. P Debye, (1945) *"Polar Molecules"* (New York : Dover)
93. H Frohlich, (1949) *"Theory of Dielectrics"* (Oxford : Clarendon)
94. K Takahashi, S Shimomura, A Nagasawa, M Ohta and K Kakegawa, *Jpn. J. Appl. Phys Lett.* 26 (1987) L1991
95. R Xu, H Xheng and J D Mackenzie, *The foruth Int. Conf. Ultrastructure Processing on glasses, ceramics and composites, Tuscon*, USA, Feb. 1987 (to be published in *J. Non-Cryst. Solids*)
96. S Jin, T H Tiefel, R C Sherwood, G W Kammlott and S M Zahurak, *Appl. Phys. Lett.* 51 (1987) 943
97. M Miijak, E Babic, A Hamzic, G Bratina and Z Marohnic, *Sup. Sci. and Tech.* 1 (1988) 141
98. R L Meng, C Kinalidis, Y Y Sun, L Gao, Y K Tao, P H Hor and C W Chu, *Nature* 345 (1990) 326
99. T Komatsu, H Meguro, R Sato, O Tanaka, K Matsusita and T Yamashita, *Jpn. J. Appl. Phys: Letts.* 27 (1988) L2063
100. Y Masuda, Y Ogawa and A J Ikushima, *Jpn. J. Appl. Phys. Letts.* 27 (1988) L1417
101. T Komatsu, R Sato, C Hirose, K Matsusita and T Yamashita, *Jpn. J. Appl. Phys. Letts.* 17 (1988) L2293
102. L Zhi and M Persson, *Sup. Sci. Tech.* 1 (1988) 198
103. H W Eeumuller and G Ries, *Physica* C160 (1989) 471
104. A Goncalves, I C Santos, M Almeida, M O Figueiredo, F Costa, J M Vieira, J M Alves and M M Godinho, *Physica* C159 (1989) 272
105. S Molla, K K Som, K Bose and B K Chaudhuri, *Phys. Rev.* B (1992) in press
106. K K Som, S Molla, K Bose, A Chakravorty and B K Chaudhuri, *Phys. Rev* B (1992) in press.
107. T Kawai, T Horiuchi, K Mitsui, K Ogura, S Takagi and S Kawai, *Physica* C161 (1991) 561